Why, when and how should exposure be considered at the within-host scale? A modelling contribution to PRRSv infection

Natacha Go, Catherine Belloc, Caroline Bidot, Suzanne Touzeau

Mathematical Medicine and Biology: A Journal of the IMA, accepted version (2018)
doi: 10.1093/imammb/dqy005

Why, when and how should exposure be considered at the within-host scale? A modelling contribution to PRRSv infection

NATACHA GO[†,‡,¶*], CATHERINE BELLOC[†], CAROLINE BIDOT[‡], SUZANNE TOUZEAU[§,‖]

[†] *BIOEPAR, INRA, Oniris, LUNAM Université, Nantes, France*
[‡] *MaIAGE, INRA, Université Paris-Saclay, Jouy-en-Josas, France*
[§] *ISA, INRA, CNRS, Université Côte d'Azur, France*
[‖] *BIOCORE, Inria, INRA, CNRS, UPMC Université Paris 06, Université Côte d'Azur, France*

[Received on 11 January 2017; revised on 22 March 2018; accepted on 11 April 2018]

Abstract

Understanding the impact of pathogen exposure on the within-host dynamics and its outcome in terms of infectiousness is a key issue to better understand and control the infection spread. Most experimental and modelling studies tackling this issue looked at the impact of the exposure dose on the infection probability and pathogen load, very few on the within-host immune response. Our aim was to explore the impact on the within-host response not only of the exposure dose, but also of its duration and peak, for contrasted virulence levels. We used an integrative modelling approach of the within-host dynamics at the between-cell level. We focused on the Porcine Reproductive and Respiratory Syndrome virus (PRRSv), a major concern for the swine industry. We quantified the impact of exposure and virulence on the viral dynamics and immune response by global sensitivity analyses and descriptive statistics. We found that the area under the viral curve, an indicator of the infection severity, was fully determined by the exposure intensity. The infection duration increased with the strain virulence and, for a given strain, exhibited a positive linear correlation with the exposure intensity logarithm and the exposure duration. Taking into account the exposure intensity is hence necessary. Besides, representing the exposure due to contacts by a single punctual dose would tend to underestimate the infection duration. As the infection severity and duration both contribute to the pig infectiousness, a prolonged exposure of the adequate intensity would be recommended in an immuno-epidemiological context.

Keywords: PRRSv, exposure, strain virulence, within-host dynamics, mathematical model

1. Introduction

Exposure of susceptible individuals is determined by the host contact structure, as well as the density and infectiousness of infected individuals. Together with host susceptibility and pathogen virulence, exposure first determines the host infection probability. Then, in case of successful infection, they drive the within-host infection and immune dynamics. In turn, the within-host dynamics dictates the morbidity and mortality of the host, as well as its infectiousness. Besides, the within-host dynamics determines the memory immunity and hence the host protection to a secondary challenge. Understanding the impact of exposure on the within-host dynamics is hence a key issue (Li & Handel, 2014; Marois *et al.*, 2012; Steinmeyer *et al.*, 2010).

Porcine Respiratory and Reproductive Syndrome virus (PRRSv), a major concern for the swine industry (Darwich *et al.*, 2010; Zimmerman *et al.*, 2006), is of particular interest in this context. Firstly, PRRSv within-host dynamics varies considerably according to the strain virulence and host susceptibility, but the underlying mechanisms are only partially understood (Murtaugh & Genzow, 2011; Kimman *et al.*, 2009; Lunney & Chen, 2010; Thanawongnuwech & Suradhat, 2010). As PRRSv mainly targets

*Corresponding author: natacha.go@laposte.net

pulmonary macrophages, a key component of the innate immune response, it alters the whole immune response. Secondly, the influence of exposure on PRRSv within-host dynamics is unknown. A few experimental studies explored the effect of exposure route and dose on PRRSv infection probability (Hermann *et al.*, 2005; Yoon *et al.*, 1999). Studies on other viruses showed that the inoculum dose determines the within-host immune dynamics and course of infection (Li & Handel, 2014; Marois *et al.*, 2012). However, no such study was conducted for PRRSv. To address this gap, we studied the impact of exposure dose and duration on the within-host dynamics for contrasted levels of strain virulence.

We tackled this issue by a mechanistic modelling approach at the host level. We based our study on an integrative model of PRRSv within-host dynamics that represents the immune mechanisms at the between-cell scale and integrates the heterogeneous knowledge on PRRSv (Go *et al.*, 2014). In this previous work, we had identified the immune mechanisms that determine the infection duration depending on the strain virulence. However, we only considered the infection by a *single punctual dose*, defined as an instantaneous intake of a viral dose. A punctual dose either corresponds to an experimental inoculation of isolated pig or to a single contact with an infected pig under natural conditions. Approximating exposure by a punctual dose is common in experimental infections (Marois *et al.*, 2012; Hermann *et al.*, 2005), within-host models (Li & Handel, 2014), and immuno-epidemiological models (Pepin *et al.*, 2010; Mideo *et al.*, 2008; Steinmeyer *et al.*, 2010; Martcheva, 2011; Gandolfi *et al.*, 2014). However, infection may results from repeated contacts with infected individuals, so exposure duration as well as exposure dose should be taken into account. Consequently, we represented exposure in our model by bell-shaped time-dependent functions characterised by their duration and intensity, the latter corresponding to the total viral dose received through exposure. Low pathogen intakes might or might not result in infection (Ben-Ami *et al.*, 2010; Pujol *et al.*, 2009). We focused in this paper on successful infections, so this random outcome does not need to be reproduced by our model, and we chose the exposure intensities accordingly from experimental inoculum doses.

In this paper, we first give an overview of the within-host model and define the designs of numerical experiments built to explore the impact of virulence level, exposure intensity and duration on characteristics of the viral and immune dynamics. We then quantify their impact by global sensitivity analyses and descriptive statistics. We assess the errors made on the various characteristics when approximating exposure by simplified functions. Finally, we discuss our results, highlighting the impact of exposure on the between-host dynamics and suggesting when and how to take exposure into account.

2. Materials and methods

2.1. Model

We used a model of the within-host dynamics representing the immune mechanisms at the between-cell scale (Go *et al.*, 2014). This integrative approach takes into account the heterogeneous knowledge on PRRSv and represents the whole immune response. It is based on an extensive literature review (Go, 2014, Chap. 1). Experimental studies on respiratory pathogens provided a generic framework (Rouse & Sehrawat, 2010; Braciale *et al.*, 2012; Coquerelle & Moser, 2010; Borghetti, 2005; Bosch *et al.*, 2013; Kidd, 2003; LeRoith & Ahmed, 2012; Knosp & Johnston, 2012). Experimental studies on PRRSv infection are highly heterogeneous (Darwich *et al.*, 2010, 2011; Kimman *et al.*, 2009; Lunney & Chen, 2010; Mateu & Díaz, 2008; Murtaugh & Genzow, 2011; Nauwynck *et al.*, 2012; Thanawongnuwech & Suradhat, 2010; Zimmerman *et al.*, 2006, reviews). They showed that (i) PRRSv infection hampers the whole immune response and (ii) depending on the strain virulence and pig susceptibility, different mechanisms have been identified as determining the infection severity and duration. The main ones are: (i) the target cell permissiveness and viral replication rate; (ii) the cytokine levels of antiviral (TNF_α, IFN_α and IFN_γ) and immuno-regulatory, either pro-cellular (IL_{12} and IFN_γ) or pro-humoral (IL_{10} and TGF_β); (iii) the balance between the adaptive response sub-types: cellular (cytotoxic lymphocytes and IFN_γ), humoral (antibodies and IL_{10}) and regulatory (TGF_β and IL_{10}) responses (Murtaugh & Genzow, 2011; Kimman *et al.*, 2009; Lunney & Chen, 2010; Thanawongnuwech & Suradhat, 2010, reviews).

Published models are either global but with few explicit mechanisms, or detailed but with a partial view of the within-host dynamics, be it for PRRSv (Doeschl-Wilson & Galina-Pantoja, 2010) or related

pathogens, such as *Mycobacterium tuberculosis* (Marino *et al.*, 2011; Gammack *et al.*, 2005, reviews) and influenza viruses (Dobrovolny *et al.*, 2013; Beauchemin & Handel, 2011; Smith & Perelson, 2011; Murillo *et al.*, 2013, reviews). None of them provides a comprehensive representation of the multiplex immune response affecting host-pathogen interactions during PRRSv infection. So we integrated in our model: (i) an explicit and detailed representation of the innate immune mechanisms; (ii) the orientation of the adaptive response towards the cellular, humoral and regulatory responses; (iii) an explicit representation of the main cytokines and their complex regulations of the immune mechanisms. We did not include the memory response, as we only considered PRRSv-naive pigs at the post-weaning stage, *i.e.* with no infectious past and with a fully competent immune system. The functional diagram of the model appears in Fig. 1.

We used a deterministic modelling framework, as we assumed that the within-host variability observed among infected hosts is mainly due to variations in strain virulence and host susceptibility, which are captured in our model parameters.

Subsection 2.1.1 describes the main components of the model, illustrated by a few representative equations. Our modelling assumptions are detailed and justified in the Supplementary material, which gives a complete description of the model and the corresponding equations. Subsection 2.1.2 presents the model calibration, based on our previous paper (Go *et al.*, 2014), and subsection 2.1.3 specifies the initial conditions used in the simulations.

2.1.1. Model overview The deterministic dynamic model consists of 14 ordinary differential equations that describe the evolution over time of the 14 state variable concentrations (Fig. 2). It is a slightly simplified version of our previous model (Go *et al.*, 2014): we grouped some state variables[1] and simplified the cytokine regulation functions. These simplifications had little impact on the model behaviour (**Figure A2**, Supplementary material).

Exposure to PRRSv is defined as the virus intake per time unit and it is represented by a time-dependent function $E(t)$. It initiates the infection and the immune response. When a free viral particle encounters a susceptible macrophage, it can either be phagocyted, resulting in viral destruction, or it can infect the cell, resulting in viral multiplication. The phagocytosis (rate η) is amplified by antiviral cytokines (A_i and IFN_γ) and inhibited by immuno-modulatory cytokines. The infection (rate β) is amplified by IL_{10} and inhibited by A_i and TGF_β. Phagocyting macrophages revert to a susceptible status after viral destruction (rate γ); it is amplified by the antiviral cytokines and inhibited by IL_{10}. The excretion (rate e), representing the result of the replication within the cell and the release of free viral particles outside the cell, is inhibited by antiviral cytokines. Pro-inflammatory cytokines amplify the recruitment of susceptible macrophages (inflow A_m) and natural killers. Macrophages undergo natural decay (rate μ_M^{nat}) and TNF_α-induced apoptosis (rate μ_M^{ap}). Infected macrophages are cytolysed by natural killers (rate μ_M^{inn}) and cellular effectors (rate μ_M^{ad}). The viral particles undergo natural decay (rate μ_V^{nat}) and are neutralised by the humoral response (rate μ_V^{ad}). Corresponding equations (susceptible macrophage and viral dynamics) are:

$$
\begin{aligned}
\dot{\mathrm{M}}_S = {} & A_m\,[1+\kappa^+(\mathrm{P}_i\ \mathrm{IL}_{12})] && \longleftarrow \text{recruitment} \\
& -\eta\ \mathrm{M}_S\ V\ \kappa^-(\mathrm{IL}_{10}+\mathrm{TGF}_\beta)\ [1+\kappa^+(\mathrm{A}_i+\mathrm{IFN}_\gamma)] && \longleftarrow \text{phagocytosis} \\
& +\gamma\ \mathrm{M}_P\ \kappa^-(\mathrm{IL}_{10})\ [1+\kappa^+(\mathrm{A}_i+\mathrm{IFN}_\gamma)] && \longleftarrow \text{end of phagocytosis} \\
& -\beta\ \mathrm{M}_S\ V\ \kappa^-(\mathrm{A}_i+\mathrm{TGF}_\beta)\ [1+\kappa^+(\mathrm{IL}_{10})] && \longleftarrow \text{infection} \\
& -\mathrm{M}_S\ [\mu_M^{\mathrm{nat}}+\mu_M^{\mathrm{ap}}\ \kappa^+(\mathrm{A}_i)] && \longleftarrow \text{decay}
\end{aligned}
\tag{2.1}
$$

[1]The "latent" and "excreting" macrophage states in (Go *et al.*, 2014) are merged into an "infected" state; the 3 pro-inflammatory cytokines are merged into 1 functional group (P_i); the 2 innate antiviral cytokines are merged into 1 functional group (A_i). See the Supplementary material for more details.

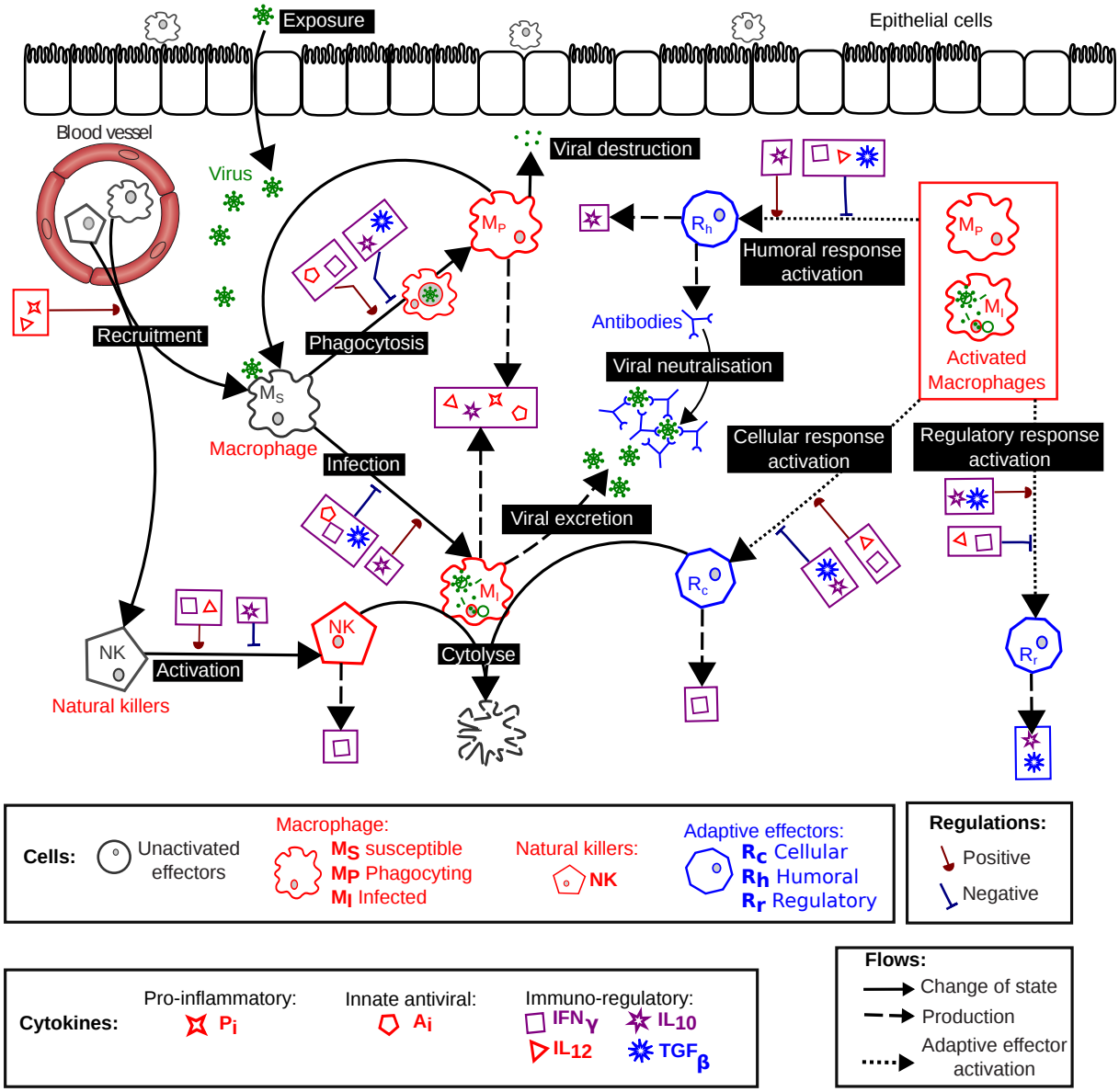

FIG. 1. **Functional diagram of the immune response to PRRSv infection.** *Exposure* to the virus initiates the within-host dynamics. Interactions between macrophages and virus result in macrophage activation by either *phagocytosis* (amplified by antiviral cytokines and inhibited by immuno-modulatory cytokines) or macrophage *infection* (amplified by immuno-modulatory cytokines and inhibited by antiviral cytokines) resulting in the viral *excretion*. The activated macrophages initiate the adaptive response. The adaptive response orientation depends on the cytokine environment: IFN_γ and IL_{12} promote the *cellular response*, whereas immuno-modulatory cytokines promote the *humoral* and *regulatory responses*. The cellular response and the natural killers are responsible for the destruction of infected cells by *cytolysis*. The humoral response is responsible for the *viral neutralisation* through antibodies. The *recruitment* of susceptible macrophages and natural killers is amplified by the pro-inflammatory cytokines. Colour code: virus in green, innate components in red, adaptive components in blue, components belonging both to the innate and adaptive responses in purple.

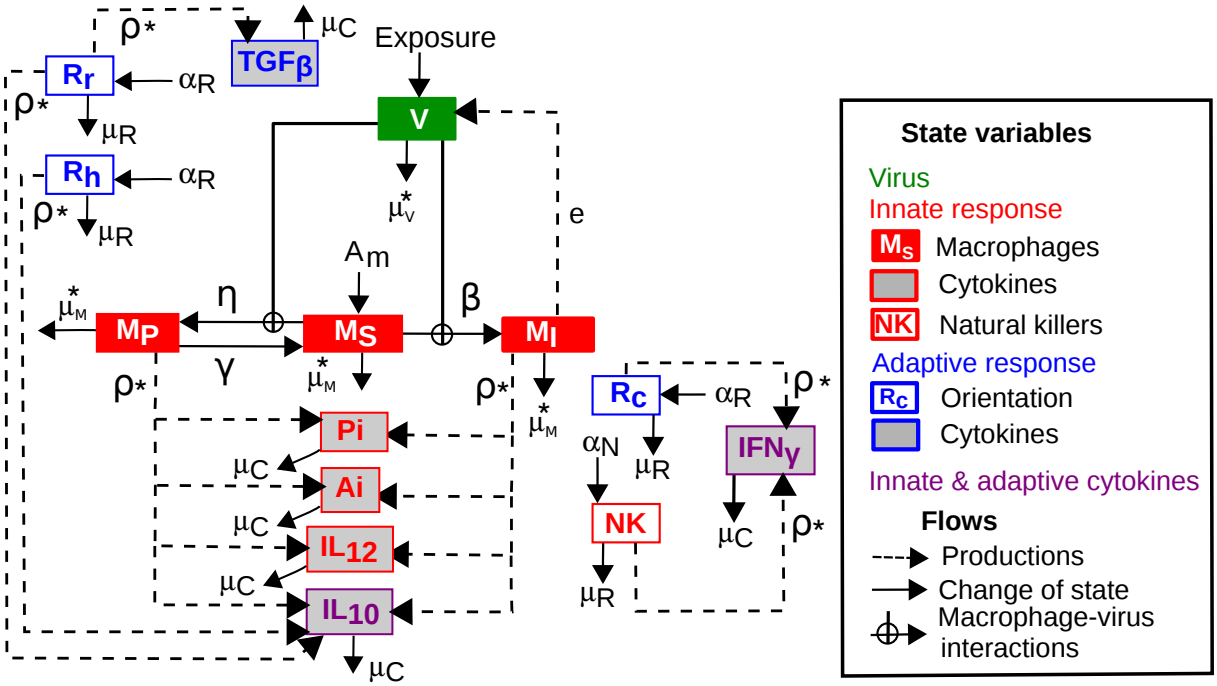

FIG. 2. **Scheme of the model: state variables and flows (without regulations)**. The state variables consist of: the free viral particles (V); the susceptible (M_S), phagocyting (M_P) and infected (M_I) macrophages; the natural killers (NK); the cellular (R_c), humoral (R_h) and regulatory (R_r) adaptive effectors; the pro-inflammatory cytokines (P_i), the innate antiviral cytokines (A_i) and the immuno-regulatory cytokines (IL_{12}, IFN_γ, IL_{10} & TGF_β). The flows represented are: the viral exposure $E(t)$; the recruitment of susceptible macrophages (A_m); the activation of natural killers (α_R) and cells of the adaptive response (α_R); the decay of the free viral particles (μ_V), the macrophages (μ_M*), the natural killers (μ_N), the adaptive cells (μ_R) and the cytokines (μ_C); the macrophage state changes, *i.e.* phagocytosis (η and γ) and the infection (β); the excretion of free viral particles by infected macrophages (e) and the cytokine syntheses by activated immune cells (ρ*). For the sake of readability, the cytokine and cell regulations are not drawn and some parameter notations (marked with $*$) are simplified.

$$
\begin{aligned}
\dot{\mathrm{V}} = {} & E(t) && \longleftarrow \text{exposure} \\
& - \eta\, \mathrm{M}_S\, \mathrm{V}\, \kappa^-(\mathrm{IL}_{10} + \mathrm{TGF}_\beta)\, [1 + \kappa^+(\mathrm{A}_i + \mathrm{IFN}_\gamma)] && \longleftarrow \text{phagocytosis} \\
& - u\, \beta\, \mathrm{M}_S\, V\, \kappa^-(\mathrm{A}_i + \mathrm{TGF}_\beta)\, [1 + \kappa^+(\mathrm{IL}_{10})] && \longleftarrow \text{infection} \\
& + e\, \mathrm{M}_I\, \kappa^-(\mathrm{A}_i + \mathrm{IFN}_\gamma) && \longleftarrow \text{excretion} \\
& - \mathrm{V}\, [\mu_{\mathrm{V}}^{\mathrm{nat}} + \mu_{\mathrm{V}}^{\mathrm{adap}}\, \mathrm{R}_h] && \longleftarrow \text{decay \& neutralisation}
\end{aligned}
\tag{2.2}
$$

Cytokines drive the model dynamics by a complex feedback system, as illustrated in Fig. 1. We selected the cytokines that better represent the pro-inflammatory, antiviral and immuno-regulatory functions. The cytokine dynamics consist of two steps: synthesis by activated innate and adaptive cells and decay. The synthesis can be regulated by cytokines. Cytokine regulations (up κ^+ and down κ^-) depend on the cytokine concentrations (C_i) and are based on the Michaelis–Menten function (Gammack *et al.*, 2005; Marino *et al.*, 2010; Wigginton & Kirschner, 2001):

$$\kappa^+(C_i) = \frac{v_m\, C_i}{k_m + C_i}; \quad \kappa^-(C_i) = \frac{k_m}{k_m + C_i}.$$

A given rate (r) can either be activated ($r\ \kappa^+(C_i)$), amplified ($r\ [1 + \kappa^+(C_i)]$) or inhibited ($r\ \kappa^-(C_i)$) by a cytokine. Regulations often involve several cytokines (C_i and C_j), which can act independently ($\kappa(C_i + C_j)$) or in synergy ($\kappa(C_i\, C_j)$).

We represented the adaptive response by three effectors corresponding to the cellular R_c, humoral R_h and regulatory R_r responses (Fig. 1). The adaptive response orientation depends on the immuno-regulatory cytokines. The dynamics of each effector consists of three steps: activation by activated macrophages (phagocyting or infected), proliferation and decay. R_c synthesises IFN_γ and destroys infected macrophages. R_h synthesises IL_{10} and neutralises free viral particles through antibodies. R_r synthesises IL_{10} and TGF_β.

2.1.2. Model calibration The model calibration consisted in the definition of a reference scenario, representing the infection of a PRRSv-naive pig at the post-weaning stage, with an intermediate susceptibility, by a moderately virulent PRRSv strain. The parameter values are based on our previous published study (Go *et al.*, 2014). As both models in this and our previous study slightly differ, a few parameters had to be updated. Details are given in the Supplementary material: in particular, the updated parameter values are given in **Table A4** and model variables are compared between both models in **Figure A2**.

2.1.3. Simulations We simulated the infection of a PRRSv-naive pig at the post-weaning stage, *i.e.* with no maternal antibodies, during 300 days. The initial conditions were set as follows: $\mathrm{M}_S(0) = 5\,10^5$cells/ml for the susceptible macrophages and all remaining variables were set to zero. The model was implemented in Scilab 5.3.3[2].

2.2. Exposure functions

We represented natural and experimental PRRSv exposures (*i.e.* the virus intake per time unit) by way of bell-shaped functions, characterised by their duration, intensity and peak. We identified three kinds of exposure: short (E_s) and prolonged (E_p) simple exposures, as well as a combination of the two (E_{s+p}).

2.2.1. Simple exposures

SHORT EXPOSURE (E_s) It represents an experimental infection by a single inoculation of an isolated pig. Lymphoid tissues and lungs become infected 12 to 24 hours post experimental inoculation (Zimmerman *et al.*, 2006; Murtaugh, 2005). Short exposure can also be due to a single contact with an infected pig under natural conditions. In both cases, viral particles have then to migrate to the lungs and are exposed to the first line of defence of the organism (physical barriers and epithelial cells), which slow

[2] `Scilab`, Open source software for numerical computation. http://www.scilab.org/

down their progression. So we chose to represent a short exposure by a narrow bell-shaped input of viral particles that lasts for one day.

PROLONGED EXPOSURE (E_p) It represents an infection by repeated contacts with infected pigs. When PRRSv is introduced in a batch of susceptible pigs, it spreads rapidly. The resulting outbreak is often associated with a bell-shaped prevalence curve describing the evolution over time of the proportion of infected individuals in the batch (Zimmerman *et al.*, 2006). Given the high frequency of contacts within a batch, representing exposure to infected individuals by a smooth bell-shaped function is an approximation that we deemed reasonable. It is also appropriate in an experimental setting, where susceptible animals are in contact with inoculated pigs. Indeed, the infectiousness of a PRRSv-infected pig is strongly correlated with its viremia, which follows a bell-shaped curve throughout the infection duration (Charpin *et al.*, 2012).

Infectiousness is shorter than the infection duration (Charpin *et al.*, 2012). PRRSv mean infection duration in the lung is 56 days (Zimmerman *et al.*, 2006), so the exposure duration should not exceed 50 days.

Experimental data show that the viral peak occurs between 7 and 14 days post-inoculation (Zimmerman *et al.*, 2006). No such data were available for natural infections, so we assumed that viral peaks were fairly similar in both experimental and natural cases. The exposure peak should not occur after the viral peak, so we set the former at 7 days. It is consistent with the the literature for inoculated pigs, as well as pigs infected by contacts (Charpin *et al.*, 2012).

REPRESENTATION To represent the simple exposures (short and prolonged), we chose a function of time $E(t)$, expressed in $\text{TCID}_{50/\text{ml}}\,\text{day}^{-1}$ [3], based on the Beta distribution (Fig. 3):

$$E(t) = \begin{cases} \mathcal{N}_E \, \dfrac{t^{a-1}\,(D_E - t)^{b-1}}{\int_0^{D_E} t^{a-1}\,(D_E - t)^{b-1}\,dt} & \text{if } 0 < t < D_E \\ 0 & \text{else} \end{cases} \tag{2.3}$$

with
$1 < a < b$	shape parameters (no unit) for a left-shifted bell-shaped curve,
$\mathcal{N}_E$	exposure intensity (in $\text{TCID}_{50/\text{ml}}$),
D_E	exposure duration (in days).

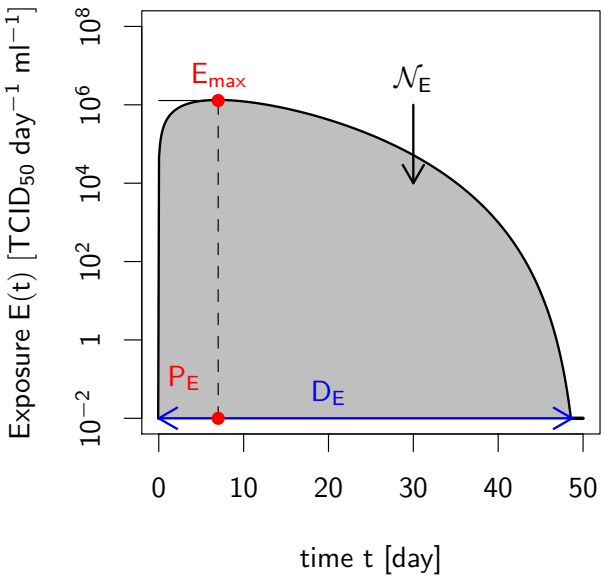

FIG. 3. **Simple exposure function (semi-log graph) and its characteristics.** Exposure to the virus is a function of time $E(t)$ defined in Equation (2.3). It is characterised by the exposure peak $E_{\max}$, the exposure peak date P_E, the exposure duration D_E and the exposure intensity $\mathcal{N}_E$ (AUC).

[3] $\text{TCID}_{50/\text{ml}}$, the median Tissue Culture Infective Dose, is the usual unit for the viral load.

The exposure intensity or dose $\mathcal{N}_E$ was defined as the total number of viral particles received through exposure, corresponding to the area under the curve (AUC). It varied between $10^{4.3}$ and $10^{9.3}$ $\text{TCID}_{50/\text{ml}}$, as reported in experimental inoculations (Johnson *et al.*, 2004). The exposure duration D_E was set depending on the exposure type: $D_E = 1$ for short exposures and for prolonged exposures $10 \leq D_E \leq 50$ (justified above). The curve peaks at: $P_E = \frac{D_E(a-1)}{a+b-2}$, which was set to 0.35 day for E_s and 7 days for E_p (see above). The higher the b (resp. a), the flatter the curve at the end (resp. at the beginning) of the exposure. We set b in order to obtain a rather flat curve at the end: for prolonged exposures, we set $E(D_E - 1) \simeq 0.01$ $\text{TCID}_{50/\text{ml}}$ day^{-1}; for the short one-day exposure, we chose $b = 5$. We deduced a from P_E and b: $a = \frac{P_E\,(b-2)+D_E}{D_E-P_E}$.

2.2.2. Combined exposures A combined exposure correponds to an experimental infection of non-isolated pigs. The combined exposure is the sum of the corresponding simple exposure functions: $E_{s+p} = E_s + E_p$. It is therefore characterised by an exposure duration $D_{E_{s+p}} = D_{E_p}$ and by an exposure intensity $\mathcal{N}_{E_{s+p}} = \mathcal{N}_{E_s} + \mathcal{N}_{E_p}$ that also corresponds to the total exposure intensity received.

2.3. Designs of numerical experiments

We tested three virulence levels: low (S_1), reference (S_2) and high (S_3). Highly virulent strains are assumed to (i) efficiently infect the cells and replicate, (ii) promote the host capacity to synthesise immunomodulatory cytokines while reducing the host capacity to synthesise antiviral cytokines and (iii) reduce the activation of the adaptive response (Gómez-Laguna *et al.*, 2013; Murtaugh & Genzow, 2011; Gimeno *et al.*, 2011). So we defined low and high virulence levels S_vir by varying $\pm 35\%$ the reference values for the parameters related to (i) the macrophage permissiveness (e, η and β), (ii) the cytokine synthesis rates ($\rho^{\text{inn}}_{\text{IFN}_\gamma}$, $\rho^{\text{ad}}_{\text{IFN}_\gamma}$, $\rho^{\text{inn}}_{\text{IL}_{10}}$, $\rho^{\text{ad}}_{\text{IL}_{10}}$, ρ_{TGF_β}) and (iii) the rate of adaptive response activation (α_R). The corresponding values are given in Table 1.

TABLE 1. **Model parameter values for the three virulence levels used in designs $\mathbf{D_1}$ and $\mathbf{D_2}$.** The reference value (ref.) corresponds an intermediate virulence level (see Table **A3**). Parameter involved in the virulence level are linked to the *macrophage permissiveness* (excretion rate e, phagocytosis rate η and infection rate β); the *synthesis capacity* of antiviral cytokines (innate ρ_{A_i} or adaptive IFN_γ by natural killers $\rho^{\text{inn}}_{\text{IFN}_\gamma}$ or cellular effectors $\rho^{\text{ad}}_{\text{IFN}_\gamma}$) and immuno-modulatory cytokines (IL_{10} by macrophages $\rho^{\text{inn}}_{\text{IL}_{10}}$ or humoral and regulatory effectors $\rho^{\text{ad}}_{\text{IL}_{10}}$); the *activation level of adaptive response* α_R.

	e	η	β	ρ_{A_i}	$\rho^{\text{inn}}_{\text{IFN}_\gamma}$	$\rho^{\text{ad}}_{\text{IFN}_\gamma}$	$\rho^{\text{inn}}_{\text{IL}_{10}}$	$\rho^{\text{ad}}_{\text{IL}_{10}}$	ρ_{TGF_β}	α_R
low S_1	0.13	$6.75\,10^{-7}$	$0.35\,10^{-6}$	0.0675	13.5	13.5	0.013	1.3	6.5	$1.35\,10^{-5}$
ref. S_2	0.2	$5\,10^{-7}$	10^{-6}	0.05	10	10	0.02	2	10	10^{-5}
high S_3	0.27	$3.25\,10^{-7}$	$1.35\,10^{-6}$	0.0325	6.5	6.5	0.027	2.7	13.5	$0.35\,10^{-5}$
units	e : [V][Ce]$^{-1}$day^{-1}		η, β : [Ce]$^{-1}$day^{-1}		ρ. : [Cy][Ce]$^{-1}$day^{-1}			α_R : day^{-1}		

We tested six exposure durations D_E (one short s and five prolonged $p_1, \ldots, p_5$) and six graduated levels of exposure intensity $\mathcal{N}_E$ ($L_1, \ldots, L_6$) given in Table 2. Each simple exposure function is denoted by $E^{\mathcal{N}_E}_{D_E}$. We defined a first complete design $\mathbf{D_1}$ for the simple exposures crossing the six exposure durations D_E, the six exposure intensities and the three virulence levels S_vir (Fig. 4).

For the combined exposures E_{s+p}, we defined a second complete design $\mathbf{D_2}$ (Fig. 4): first we crossed two D_{E_p} durations (p_1 and p_5) with three exposure intensities $\mathcal{N}_{E_p}$ (L_1, L_4, L_6); then we combined them with the same three intensities $\mathcal{N}_{E_s}$ for the short exposure; finally we crossed these 18 exposure scenarios with the three virulence levels. Each combined exposure function is denoted by $E^{\mathcal{N}_{E_s}+\mathcal{N}_{E_p}}_{D_{E_s}+D_{E_p}}$. Values of the combined exposure intensity are $\mathcal{N}_{E_{s+p}} = \mathcal{N}_{E_s} + \mathcal{N}_{E_p}$. They can be approximated by the highest intensity of the combination: $\mathcal{N}_{E_{s+p}} \simeq \max(\mathcal{N}_{E_s}, \mathcal{N}_{E_p})$. Illustrations of simple and combined exposure functions are shown in Fig. 5.

TABLE 2. **Exposure parameter values for the simple exposures used in design $\mathbf{D_1}$.** Parameters, defined in Equation (2.3), are the exposure intensity $\mathcal{N}_E$, the exposure duration D_E and the shape parameters a and b. a is deduced from the three other parameters and the exposure peak date P_E by: $a = \frac{P_E(b-2)+D_E}{D_E-P_E}$.

			L_1	L_2	L_3	L_4	L_5	L_6
		$\mathcal{N}_E$	$10^{4.3}$	$10^{5.3}$	$10^{6.3}$	$10^{7.3}$	$10^{8.3}$	$10^{9.3}$
D_E		P_E	b					
s	1	0.35	5	5	5	5	5	5
p_1	10	7	1.4	1.9	2.3	2.7	3.1	3.6
p_2	20	7	2.9	4.7	6.6	8.4	10.3	12.1
p_3	30	7	4.3	7.6	11	14	17	21
p_4	40	7	5.7	5.7	5.7	8.1	8.1	8.1
p_5	50	7	7.1	7.1	7.1	7.1	7.1	7.1
units		$\mathcal{N}_E$: $TCID_{50/ml}$	D_E, P_E : day			a, b : no unit		

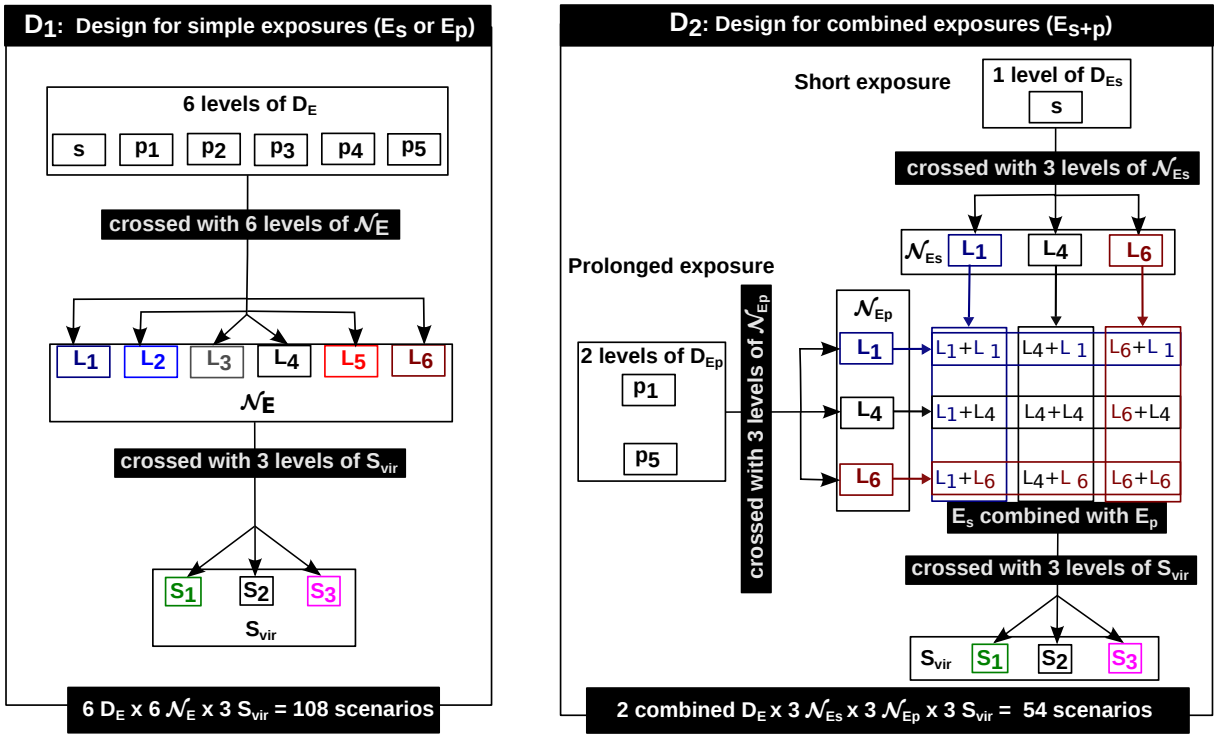

FIG. 4. **Designs of numerical experiments for the simple (design $\mathbf{D_1}$) and combined (design $\mathbf{D_2}$) exposure scenarios.** The scenarios are defined by the following parameters, considered as inputs for the global sensitivity analyses: the exposure duration $D_E \in \{s, p_1, p_2, p_3, p_4, p_5\}$; the exposure intensity $\mathcal{N}_E \in \{L_1, L_2, L_3, L_4, L_5, L_6\}$; the virulence level $S_{\text{vir}} \in \{S_1, S_2, S_3\}$.

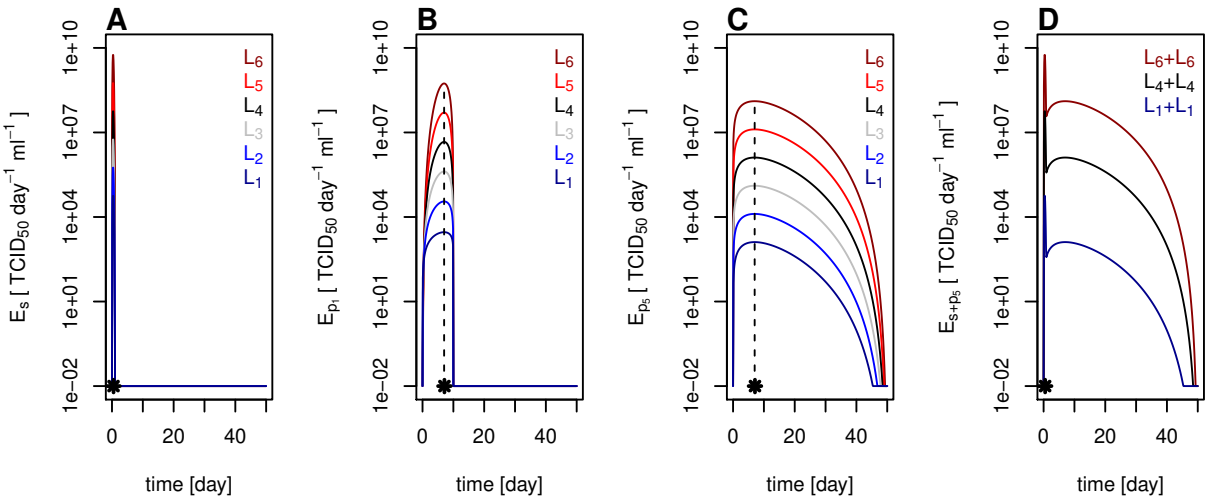

FIG. 5. **Exposure functions (semi-log graphs) used in designs $\mathbf{D_1}$ and $\mathbf{D_2}$ (selection).** The whole exposure intensity range $\mathcal{N}_E \in \{L_1, L_2, L_3, L_4, L_5, L_6\}$ and a selection of exposure durations are represented. Panels **A–C** correspond to simple exposures (design $\mathbf{D_1}$) for various durations: **A** short $D_E = s$, **B** prolonged $D_E = p_1$ and **C** prolonged $D_E = p_5$. Panel **D** corresponds to combined exposures (design $\mathbf{D_2}$) for $D_E = p_5$ and $\mathcal{N}_{E_s} = \mathcal{N}_{E_p}$. The $*$ and the dashed line mark the exposure peak date.

2.4. Characteristics of the within-host dynamics

To characterise the viral dynamics, we considered the whole viral dynamics plus five scalar descriptors based on (Li & Handel, 2014, Li and Handel, 2014): the viral peak ($V_{\max}$), the viral peak date ($T_{\max}$), the infection duration (D_I)[4], the detection duration (D_D) and the area under the viral curve (Σ_V). They are illustrated in Fig. 6. The viral peak and infection duration more or less determine the area under the viral curve, an indicator of the infection severity.

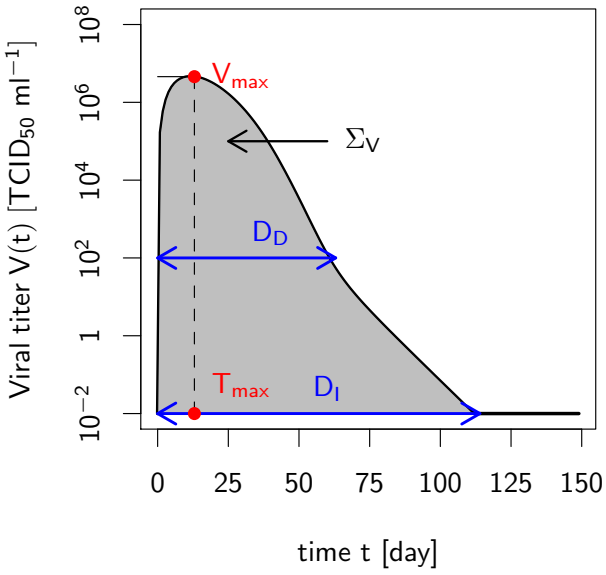

FIG. 6. **Shape and characteristics of the viral titer curve over time (semi-log graph).** The characteristics of the viral titer $\mathrm{V}(t)$ are: the viral peak $V_{\max}$, the viral peak date $T_{\max}$; the infection duration D_I, defined as the time during which $\mathrm{V}(t) > 10^{-2}$ $\mathrm{TCID}_{50/\mathrm{ml}}$; the detection duration D_D, defined as the time during which $\mathrm{V}(t)$ is higher than the detection threshold 10^2 $\mathrm{TCID}_{50/\mathrm{ml}}$ (Li & Handel, 2014); and the area under the viral curve Σ_V, defined as the cumulative number of viral particles over the simulation duration.

[4] As we used a continuous time formalism, the viral titer cannot reach the zero value in finite time. So we fixed a threshold at 10^{-2} $\mathrm{TCID}_{50/\mathrm{ml}}$ below which we assumed that the infection was resolved.

To characterise the immune response, we first chose four basic descriptors that can be measured experimentally and are relevant for PRRSv global immune response (Gómez-Laguna *et al.*, 2013; Murtaugh, 2004; Zimmerman *et al.*, 2006; Yoo *et al.*, 2010). They are based on the AUC (Area Under the Curve) of cytokines and adaptive effectors:

- Σ_{P_i}: the total pro-inflammatory cytokines (AUC), shown to be a good proxy of the activation level of the immune response (Go *et al.*, 2014) and related to the clinical status of the pig;
- $\%(\mathrm{A}_i\text{+IFN}_\gamma) = 100\ \frac{\Sigma_{\mathrm{A}_i}+\Sigma_{\mathrm{IFN}_\gamma}}{\Sigma_{\mathrm{A}_i}+\Sigma_{\mathrm{IFN}_\gamma}+\Sigma_{\mathrm{TGF}_\beta}+\Sigma_{\mathrm{IL}_{10}}}$: the percentage of anti-viral cytokines, supposed to play a key role in PRRSv infection resolution;
- $\%\mathrm{R}_c = 100\ \frac{\Sigma_{\mathrm{R}_c}}{\Sigma_{\mathrm{R}_c}+\Sigma_{\mathrm{R}_h}+\Sigma_{\mathrm{R}_r}}$: the percentage of cellular response, supposed to play a key role in PRRSv infection resolution;
- $\%\mathrm{R}_h = 100\ \frac{\Sigma_{\mathrm{R}_h}}{\Sigma_{\mathrm{R}_c}+\Sigma_{\mathrm{R}_h}+\Sigma_{\mathrm{R}_r}}$: the percentage of humoral response, supposed to play a key role in PRRSv infection persistence.

We also defined another set of five descriptors (denoted $\mathcal{N}_{\ldots/E}$) related to the destruction *vs* multiplication mechanisms of viral particles: the phagocytosis ($\mathcal{N}_{\text{pha/E}}$), neutralisation ($\mathcal{N}_{\text{neutr/E}}$) and excretion ($\mathcal{N}_{\text{excr/E}}$) of viral particles, the infection by viral particles ($\mathcal{N}_{\text{inf/E}}$) and the cytolysis of infected macrophages ($\mathcal{N}_{\text{cyt/E}}$). For each mechanism, the descriptor is defined as the ratio between the total number (AUC) of viral particles or macrophages involved and the exposure intensity ($\mathcal{N}_E$). This normalisation allowed us to compare the activation levels of the mechanisms independently from the exposure intensity. For instance, the normalised number of viral particles having infected macrophages is defined from Equation (2.2) as follows:

$$\mathcal{N}_{\text{inf/E}} = \frac{\int_{t=0}^{D_I} u\,\beta\,\mathrm{M}_S(t)\,V(t)\,\kappa^-(\mathrm{A}_i(t)+\mathrm{TGF}_\beta(t))\,[1+\kappa^+(\mathrm{IL}_{10}(t))]\,dt}{\mathcal{N}_E}.$$

2.5. Analyses

We performed all our analysis using R software[5], version 3.0.2.

2.5.1. Sensitivity analyses We aimed at exploring the influence of exposure and virulence (main effect and interactions) for simple scenarios (design $\mathbf{D_1}$) on the within-host dynamics. To do so, we performed global sensitivity analyses that allowed to quantify the influence of the scenario parameters (D_E, $\mathcal{N}_E$ and S_{vir}), considered as inputs on model outputs. The computed sensitivity indices quantify the fraction of output variance among simulations explained by each input. We quantified the scenario influence on (i) the 14 descriptors of the within-host dynamics using univariate sensitivity analyses and on (ii) the viral titer curve over time using a multivariate sensitivity analysis.

UNIVARIATE Within-host characteristics are scalar outputs so a classical univariate method is suitable. The sensitivity indices were computed using decomposition of the variance, like for Sobol's indices. We used here an ANOVA-based decomposition until the second order effect (Saltelli *et al.*, 2000; Lamboni *et al.*, 2011). The sensitivity index associated with each term (main effect or interaction) is defined as the ratio between the sum of squares corresponding to that term and the total sum of squares.

MULTIVARIATE The viral titer curve over time is not a scalar output so we used a multivariate method, based on a decomposition of the output by a principal component analysis (PCA) (Lamboni *et al.*, 2011). As a result of the PCA, an inertia proportion is attributed to each component. It represents the variability among simulations carried by the component. Moreover, each simulation is given a "score" on each component, a scalar which represents the projection of the output on the component. Sensitivity indices

[5] R, the R Project for Statistical Computing. http://www.r-project.org

are computed for each component using these scores as outputs. Finally, a generalised sensitivity index (GSI) is calculated for each term as the sum of the sensitivity indices corresponding to that term on each PCA component, weighted by the inertia of the component. We used the multisensi R package[6] for these analyses.

2.5.2. Fitting linear models on the infection duration We did a focus on an output of particular interest, the infection duration (D_I), which is one component of the infectiousness. In order to quantify the influence of the scenario parameters on the infection duration, for both designs $\mathbf{D_1}$ and $\mathbf{D_2}$, we fitted a linear model defined as follows:

$$D_I = \xi_0 + \xi_{S_{\text{vir}}} + \xi_{\mathcal{N}_E}\ \log(\mathcal{N}_E) + \xi_{D_E}\ D_E + \varepsilon$$

with ξ_0 the constant term and ε the residual variance. S_{vir} was considered as a qualitative factor, $\log(\mathcal{N}_E)$ and D_E as quantitative covariables. The parameters that were estimated were the three $\xi_{S_{\text{vir}}}$ for $S_{\text{vir}} \in \{S_1, S_2, S_3\}$, $\xi_{\mathcal{N}_E}$ and ξ_{D_E}.

2.5.3. Approximation errors of exposure scenario We used design $\mathbf{D_2}$ to investigate whether combined exposures E_{s+k}^{i+j} could be approximated by simple exposure functions. We chose two approximation types: (a) by either the short (E_s^i) or the prolonged (E_k^j) simple exposure of the combination; and (b) by a simple scenario with the highest exposure dose of the combination and either a short ($E_s^{\max(i,j)}$) or a prolonged ($E_k^{\max(i,j)}$) exposure duration. The relative error for each viral characteristic $C \in \{\Sigma_{\text{V}}, V_{\max}, T_{\max}, D_I\}$ was denoted by:

$$\Delta C_k^{i+j}(E_m^l) = \frac{C(E_{s+k}^{i+j}) - C(E_m^l)}{C(E_{s+k}^{i+j})} \quad \text{with } E_m^l \in \left\{E_s^i, E_k^j, E_s^{\max(i,j)}, E_k^{\max(i,j)}\right\} \quad \forall\, i,j \in \{L_1, L_4, L_6\}\ \&\ \forall\, k \in \{p_1, p_5\}. \tag{2.4}$$

Comparisons involved the same S_{vir} level for both scenarios.

For the 18 homogeneous scenarios ($i = j$), simple scenarios used in (a) and (b) approximations were the same ($E_s^i = E_s^{\max(i,j)}$ and $E_k^j = E_k^{\max(i,j)}$), leading to $18 \times 2 = 36$ comparisons. For the 36 heterogeneous scenarios ($i \neq j$), one of the four simple scenarios ($E_s^{\max(i,j)}$ if $\max(i,j) = i$, or $E_k^{\max(i,j)}$ if $\max(i,j) = j$) corresponded to both (a) and (b) approximations, leading to $36 \times 3 = 108$ comparisons. So a total of 144 comparisons were performed.

3. Results

3.1. Overview and confrontation with the literature

Globally, the higher the exposure dose, the higher the viral titer and the key immune outputs (Fig. 7), in agreement with the literature (Charpin *et al.*, 2012; Hermann *et al.*, 2005; Yoon *et al.*, 1999).

There is much information about viral titer in the PRRSv literature and our results are in good agreement with the data (Table 3). We compared the detection durations D_D with the experimental infection durations reported in the literature, as measurement techniques have a detection threshold *a priori* close to the value we chose (10^2 $\text{TCID}_{50/\text{ml}}$). The D_D range (15–94 days) is narrower than the infection durations reported in the literature (*ca* 28–251 days). However, the mean D_D (54 days) is close to the mean infection duration in the lung reported in experimental studies (56 days) (Zimmerman *et al.*, 2006).

By model construction, the viral load results from the viral exposure (income of viral particles inside the host) and the within-host dynamics (infection and immune mechanisms). Our results show that both exposure and within-host mechanisms have a notable influence on the viral load (Fig. 7 and **Figure A3** in the Supplementary material). While the immune components represented in our model are recognized as

[6] `multisensi`: Multivariate Sensitivity Analysis, an R package to perform sensitivity analysis on a model with multivariate outputs. http://cran.r-project.org/web/packages/multisensi/index.html

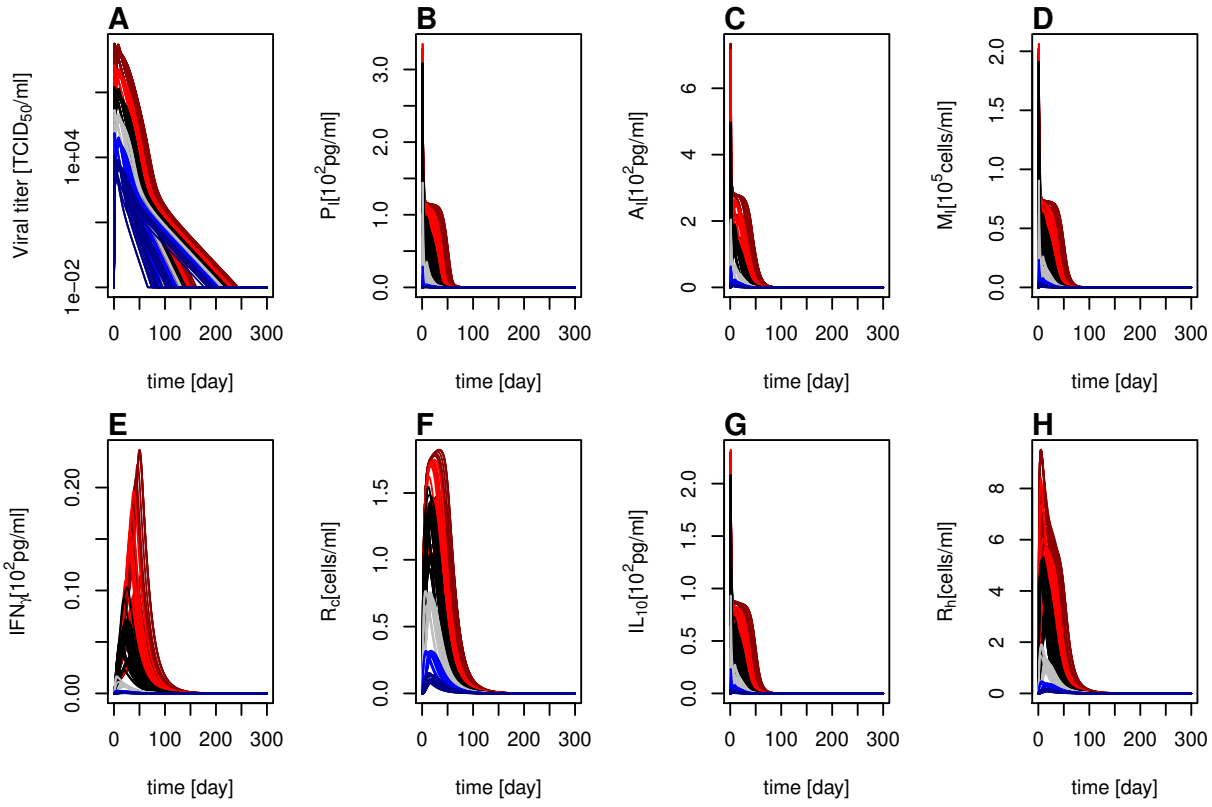

FIG. 7. **Dynamics of the viral titer and key immune outputs for all scenarios.** **A**: viral titer (semi-log graph); **B**: pro-inflammatory cytokines; **C**: innate antiviral cytokines; **D**: infected macrophages; **E**: IFN_γ cytokine; **F**: cellular effectors; **G**: IL_{10} cytokine; **H**: humoral effectors. The 108 simple (design $\mathbf{D_1}$) and 54 combined (design $\mathbf{D_2}$) exposure scenarios are represented. Exposure intensities are highlighted by colours on the graphs: $\mathcal{N}_E \in \{L_1, L_2, L_3, L_4, L_5, L_6\}$. The intensity of combined scenarios is approximated by the highest intensity of the combination (*e.g.* $L_1 + L_4 \simeq L_4$).

having a strong influence on the infection dynamics, they have been scarcely monitored in experimental studies (see review in (Go, 2014, Chap. 1)). Indeed, such titrations are very expensive and some components cannot be measured because of technical constraints. Most experimental studies focus on a few cytokines. Moreover, the monitored components, the location sample and the analysis methods vary a lot among studies. Consequently, we confronted the qualitative behaviour rather than quantitative values to the literature. Our results exhibited realistic qualitative behaviours and variation ranges (Table 3). The innate variables ($\mathrm{A}_i, \mathrm{P}_i, \mathrm{M}_I, \mathrm{IL}_{10}$ in Fig. 7) peaked in the first infection days, whereas the adaptive variables ($\mathrm{IFN}_\gamma, \mathrm{R}_c, \mathrm{R}_h$ in Fig. 7) peaked later, around two to three weeks, in agreement with the literature (Murtaugh, 2004; Darwich *et al.*, 2010; Gómez-Laguna *et al.*, 2013). As reported in the literature, our results exhibited lower percentages of cellular response than of humoral response (Table 3).

3.2. Exploring the influence of exposure and virulence

3.2.1. Viral titer dynamics The virulence level S_{vir}, the exposure dose $\mathcal{N}_E$ and exposure duration D_E explained together 90% of the variance of the whole viral dynamics (Fig. 8). In particular, 30% of the variance was explained by S_{vir} alone, 25% by $\mathcal{N}_E$ alone and 25% by the interaction between S_{vir} and $\mathcal{N}_E$, and 10% by the interaction between $\mathcal{N}_E$ and D_E. **Figure A3** in the Supplementary material highlights the non-linear relations between the viral load of the recipient and the exposure, as well as the notable influence of the within-host mechanisms on the viral dynamics.

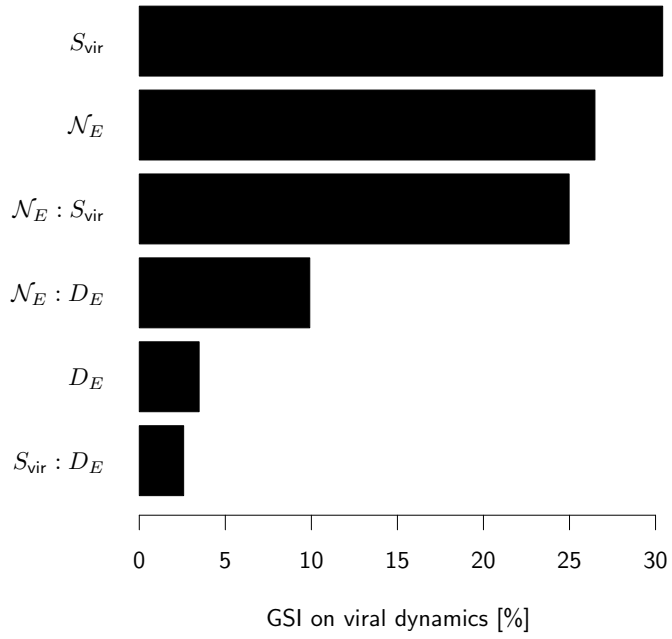

FIG. 8. **Multivariate global sensitivity analysis for the viral titer dynamics based on simple exposure scenarios (design $\mathbf{D_1}$).** Global sensitivity indices (GSI) of the virulence level S_{vir}, exposure dose $\mathcal{N}_E$ exposure duration D_E and their two-way interactions.

3.2.2. Within-host characteristics The exposure dose $\mathcal{N}_E$ had a strong and dominant influence (sensitivity indices higher than 50%) on the variance of the majority of within-host characteristics (Table 4). Exceptions were the viral peak date $T_{\max}$, the infection duration D_I and the percentage of antiviral cytokines $\%(\mathrm{A}_i\text{+}\mathrm{IFN}_\gamma)$ (Table 4). The viral peak date, $T_{\max}$, was fully determined by the exposure duration D_E (Table 4). It is linked to the contrasted exposure peak dates between the short ($P_E = 0.35$ and $T_{\max} = 1$) and prolonged exposure ($P_E = 7$ and $9 \leq T_{\max} \leq 12$) functions, as $T_{\max}$ and P_E were shown to be positively correlated. The infection duration D_I and the percentage of antiviral cytokines $\%(\mathrm{A}_i\text{+}\mathrm{IFN}_\gamma)$ were mainly determined by the virulence level and to a lesser extend by the exposure dose (Table 4). Results of particular interest are detailed below.

TABLE 3. **Summary of the viral titer and key immune outputs compared with literature data.** Minimal, median, mean and maximal values of: (i) the viral characteristics: infection D_I and detection D_D durations, viral peak $V_{\max}$ and viral peak date $T_{\max}$; (ii) the peak concentrations of key cytokines: innate antiviral A_i, pro-inflammatory P_i, IL_{10} and IFN_γ; (iii) the peak values of the cellular $\%R_c$ and the humoral $\%R_h$ effectors expressed as percentages of the sum of the three adaptive effector peaks. The infected macrophages M_I also belong to the key immune outputs but are not presented here, as the only relevant data found in the literature reported a maximal M_I number of $15\ 10^6$ cells, representing around 40% of the total macrophage concentration in the bronchoalveolar lavage fluids (Labarque *et al.*, 2003). Our results exhibited a maximal M_I percentage ranging between 0.5% and 99%, with a mean value of 42%.

	D_I	D_D	$V_{\max}$	$T_{\max}$	A_i^{peak}	P_i^{peak}	IL_{10}^{peak}	IFN_γ^{peak}	$\%R_c^{peak}$	$\%R_h^{peak}$
Model results										
min	67	15	$10^{3.5}$	1	5	0.3	0.7	0.03	9	34
median	133	60	$10^{7.2}$	10	176	96	66	4	14	46
mean	151	58	$10^{6.9}$	7	274	165	110	6	18	43
max	244	95	$10^{9.3}$	12	1002	580	580	24	33	50
References from reviews on PRRSv infection (Zimmerman *et al.*, 2006; Yoo *et al.*, 2010; Gómez-Laguna *et al.*, 2013; Murtaugh & Genzow, 2011; Darwich *et al.*, 2010). L low; H high; L/H low or high.										
tendency					L	H	H	L	L/H	L/H
mean		$\simeq 37-56$								
range		$28-251$	10^2-10^9	$7-14$	$0-10^3$	$0-10^3$	$0-10^3$	$0-10^3$		
References from PRRSv experimental infections										
(Gómez-Laguna *et al.*, 2010)		$14-{>}24$	$10^{2.3}-10^{4.5}$	14	60	75				
(Lunney *et al.*, 2010)		$\geqslant 42$	10^7	$7-14$		1600		4		
(Gimeno *et al.*, 2011)					$0-2800$		$0-1350$			
(Ait-Ali *et al.*, 2011)						1800	1000			
(Wesley *et al.*, 2006)		$22-36$	$10^{4.3}$	5				$80-120$		
(Labarque *et al.*, 2000, 2003)		$35-52$	$10^{4.5}-10^{7.3}$	7	0		$\simeq 139$			
(Liu *et al.*, 2010)		>21			600	450		100		
(Petry *et al.*, 2007)		>14	$10^{3.7}-10^{5.4}$	$4-14$				$0-328$		
Units: $D_I, D_D, T_{\max}$: day $V_{\max}$: $TCID_{50/ml}$ $A_i^{peak}, P_i^{peak}, IL_{10}^{peak}, IFN_\gamma^{peak}$: pg/ml										

TABLE 4. **Global sensitivity analyses for the within-host characteristics based on simple exposure scenarios (design $\mathbf{D_1}$).** Sensitivity indices (in %) of the virulence level S_{vir}, exposure dose $\mathcal{N}_E$ exposure duration D_E and their two-way interactions for (i) the five viral descriptors: area under the viral curve Σ_V, infection duration D_I, detection duration D_D, viral peak $V_{\max}$ and viral peak date $T_{\max}$; (ii) the four basic immune descriptors: total pro-inflammatory cytokines Σ_{Pi}, percentage of antiviral cytokines $\%(\text{A}_i\text{+IFN}_\gamma)$, percentage of cellular $\%\text{R}_c$ and $\%\text{R}_h$ humoral effectors; and (iii) the five descriptors related to immune mechanisms: normalised number of excreted viral particles $\mathcal{N}_{\text{excr/E}}$, normalised number of viral particles having infected macrophages $\mathcal{N}_{\text{inf/E}}$, normalised number of cytolysed infected macrophages $\mathcal{N}_{\text{cyt/E}}$, normalised number of neutralised viral particles $\mathcal{N}_{\text{neutr/E}}$ and normalised number of phagocyted viral particles $\mathcal{N}_{\text{pha/E}}$.

	Σ_V	D_I	D_D	$V_{\max}$	$T_{\max}$	Σ_{Pi}	$\%(\text{A}_i\text{+IFN}_\gamma)$	$\%\text{R}_c$	$\%\text{R}_h$	$\mathcal{N}_{\text{excr/E}}$	$\mathcal{N}_{\text{inf/E}}$	$\mathcal{N}_{\text{cyt/E}}$	$\mathcal{N}_{\text{neutr/E}}$	$\mathcal{N}_{\text{pha/E}}$
$\mathcal{N}_E$	100	10	82	80	0	94	19	87	86	64	80	51	97	80
S_{vir}	0	89	8	0	0	2	79	7	9	9	8	22	0	12
D_E	0	1	10	4	99	1	1	3	2	0	0	1	1	1
$\mathcal{N}_E \times S_{\text{vir}}$	0	0	0	0	0	1	1	2	3	25	11	17	1	5
$S_{\text{vir}} \times D_E$	0	0	0	0	0	0	0	0	0	0	0	0	0	0
$\mathcal{N}_E \times D_E$	0	0	0	16	0	2	0	1	1	1	0	7	1	1

Units: $D_I, D_D, T_{\max}$: day $V_{\max}$: $\text{TCID}_{50/\text{ml}}$ Σ_{Pi} : day pg/ml $\mathcal{N}_{./E}$: no unit except $\mathcal{N}_{\text{cyt/E}}$: cells/TCID_{50}

DOMINANT IMPACT OF VIRULENCE ON INFECTION DURATION We assessed the impact of exposure on the infection duration (D_I) by fitting linear models for the three virulence levels (Fig. 9). They exhibited a good fit ($R^2 > 0.98$) for the simple and combined exposure scenarios. For each virulence level, there was a linear relation between the infection duration D_I and the exposure intensity $\log(\mathcal{N}_E)$ and duration D_E. More precisely, for virulence levels $S_{\text{vir}} \in [S_1, S_3]$, we found that, after a simple exposure $D_I = [31.67, 140.82] + 9.21\ \log(\mathcal{N}_E) + 0.33\ D_E$ and after a combined exposure $D_I = [29.62, 141.12] + 9.42\ \log(\mathcal{N}_E) + 0.17\ D_E$. This finding shows that a complex interaction between the exposure and the within-host response (*i.e.* infection and immune mechanisms) determines the infection duration (see **Figure A3** in the Supplementary material).

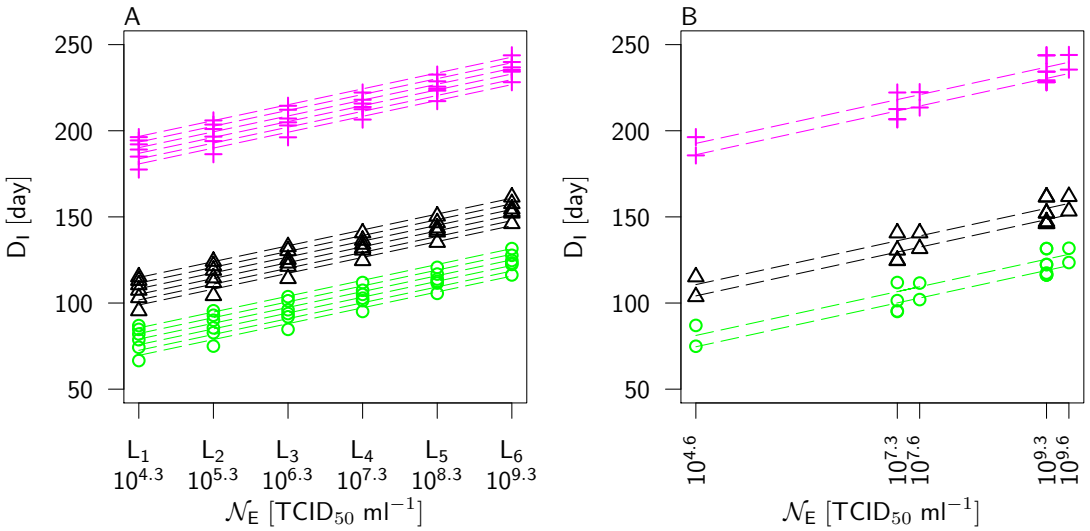

FIG. 9. **Infection duration as a linear function of the exposure dose logarithm for both designs. A**: simple exposure scenarios (design $\mathbf{D_1}$); **B**: combined exposure scenarios (design $\mathbf{D_2}$). Simulated infection durations D_I are plotted against exposure intensities $\mathcal{N}_E$ (semi-log graphs) for each virulence level $S_{\text{vir}} \in \{\circ S_1, \triangle L_2, +S_3\}$ and for each exposure duration D_E (for each S_{vir}, the higher the D_E, the higher the mark). Corresponding linear regression lines are plotted (for each S_{vir}, the higher the D_E, the higher the line).

In order to identify the underlying immune mechanisms, we used the four synthetic immune descriptors: Σ_{P_i}, $\%(\text{A}_i\text{+IFN}_\gamma)$, $\%\text{R}_c$ and $\%\text{R}_h$ (Fig. 10). High virulence levels were associated with lower percentages of antiviral cytokines $\%(\text{A}_i\text{+IFN}_\gamma)$, which resulted in longer infections (Fig. 10B.). No such trends were identified for the other descriptors. However, for each virulence level, higher levels of pro-inflammatory cytokines (Σ_{P_i}), a higher humoral response ($\%\text{R}_h$), or a lower cellular response ($\%\text{R}_c$) tended to increase the infection duration.

We highlighted two scenarios with similar infection durations, but contrasted immune dynamics (Fig. 10): median virulence and high and prolonged exposure ($Sc^- = E_{p_5}^{L_6} \times S_2$; $D_I = 162$ days) *vs.* high virulence and short and low exposure ($Sc^+ = E_s^{L_1} \times S_3$; $D_I = 176$ days). Compared to Sc^-, Sc^+ was associated with a lower Σ_{P_i}, similar $\%(\text{A}_i\text{+IFN}_\gamma)$, a higher $\%\text{R}_c$ and a lower $\%\text{R}_h$. This points out that different exposure and virulence scenarios could lead to similar infection durations but contrasted underlying immune mechanisms.

DOMINANT IMPACT OF EXPOSURE DOSE ON THREE CHARACTERISTICS The exposure dose explained more than 90% of the variance of three within-host characteristics (Table 4): the higher the exposure dose, the higher the area under the viral curve Σ_V, the total pro-inflammatory cytokines Σ_{P_i} and the normalised number of viral particles neutralised $\mathcal{N}_{\text{neutr/E}}$ (Fig. 11A, D, K). Σ_V followed a linear relationship with the exposure dose while Σ_{P_i} and $\mathcal{N}_{\text{neutr/E}}$ did not (Fig. 11A, D, K). In particular, the area under the viral curve, which is an indicator of the infection severity, increased with the total pro-inflammatory cytokines (Fig. 11A, D).

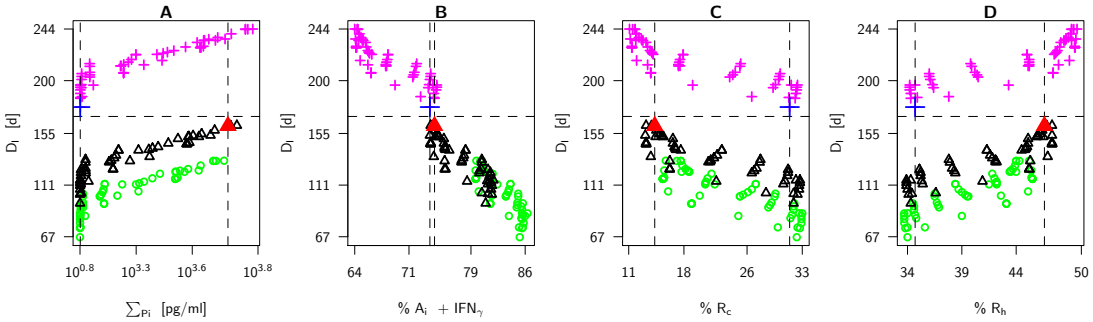

FIG. 10. **Infection duration as a function of the global immune characteristics for all scenarios. A**: total pro-inflammatory cytokines Σ_{P_i}; **B**: percentage of antiviral cytokines among innate antiviral and immuno-regulatory cytokines $\%(A_i\text{+IFN}_\gamma)$; **C**: percentage of cellular response among all adaptive effectors $\%R_c$ and **D**: percentage of humoral response among all adaptive effectors $\%R_h$. Virulence levels are highlighted by colours on the graphs: $S_{vir} \in \{\circ S_1, \triangle L_2, +S_3\}$. Scenarios of particular interest: • corresponds to $Sc^- = E_{p_5}^{L_6} \times S_2$ and + corresponds to $Sc^+ = E_s^{L_1} \times S_3$; they have similar infection durations (horizontal dashed line), but contrasted immune characteristics (vertical dashed lines), except for antiviral cytokines(**B**).

INTERACTIONS AND SATURATION EFFECTS The interaction between the two components of the exposure $\mathcal{N}_E \times D_E$ had a significant influence only on the viral peak $V_{\max}$ (Table 4, GSI=16%). As the exposure peak $E_{\max}$ is determined by the exposure dose and duration, $\mathcal{N}_E \times D_E$ corresponds to the positive impact of $E_{\max}$ on $V_{\max}$ (Fig. 11C).

The interaction between the virulence level and the exposure dose $S_{vir} \times D_E$ had no influence on none of the within-host characteristics (Table 4). Contrariwise, the interaction between the virulence level and the exposure dose $S_{vir} \times \mathcal{N}_E$ was significant for three within-host characteristics: $\mathcal{N}_{excr/E}$ (Fig. 11H), $\mathcal{N}_{inf/E}$ (Fig. 11I) and $\mathcal{N}_{cyt/E}$ (Fig. 11J). The normalised number of excreted viral particles $\mathcal{N}_{excr/E}$ (Fig. 11H) and the normalised number of infected cells $\mathcal{N}_{inf/E}$ (Fig. 11I) were negatively impacted by $\mathcal{N}_E$, while positively impacted by S_{vir}. The normalised number of cytolysed cells $\mathcal{N}_{cyt/E}$ (Fig. 11J) was positively impacted by $\mathcal{N}_E \leq \mathsf{L}_4$ and negatively impacted by $\mathcal{N}_E > \mathsf{L}_4$, while always positively impacted by S_{vir}.

Without normalisation, the excretion, infection, cytolysis, neutralisation and phagocytosis increased with $\mathcal{N}_E$ (results not illustrated). With normalisation, all but the neutralisation tended to zero for high values of $\mathcal{N}_E$, which suggests that these immune mechanisms saturated for high exposure intensities (Fig. 11H–L). Furthermore, $\mathcal{N}_{cyt/E}$ and $\mathcal{N}_{neutr/E}$ were low, suggesting that cytolysis and neutralisation had a low impact on the viral titer reduction.

3.3. Looking at the impact of exposure simplifications

3.3.1. Approximating a prolonged scenario by a short scenario We explored the errors made on the viral characteristics when approximating a prolonged exposure by a short exposure, using the results on simple exposure scenarios described above. Both short and prolonged scenarios exhibited a similar infection severity (marks confounded in Fig. 11A for each exposure intensity $\mathcal{N}_E$). However, the short exposure scenario had a shorter infection duration compared to the prolonged exposure scenario (see results above on the linear relation between D_I and D_e; Fig. 9A). Moreover, the short exposure scenario had a higher viral peak ($E_{\max}$) and an earlier viral peak date ($T_{\max}$). As short exposures were defined with an earlier (P_E) and higher exposure peak ($E_{\max}$), this last result was expected given the positive correlations between P_E and $T_{\max}$ ($R^2 = 0.99$) and the logarithms of $E_{\max}$ and $V_{\max}$ ($R^2 = 0.98$).

3.3.2. Approximating a combined scenario by a simple scenario We explored the errors made on the viral characteristics when approximating a combined exposure scenario by a simple exposure scenario. We distinguished two types of approximation. Type (a) was either the short or the prolonged simple scenario of the combination, whatever its exposure dose. Type (b) was a simple scenario with the highest exposure dose of the combination and either the short or the prolonged exposure duration. Errors on the viral characteristics due to these approximations are given in Table 5.

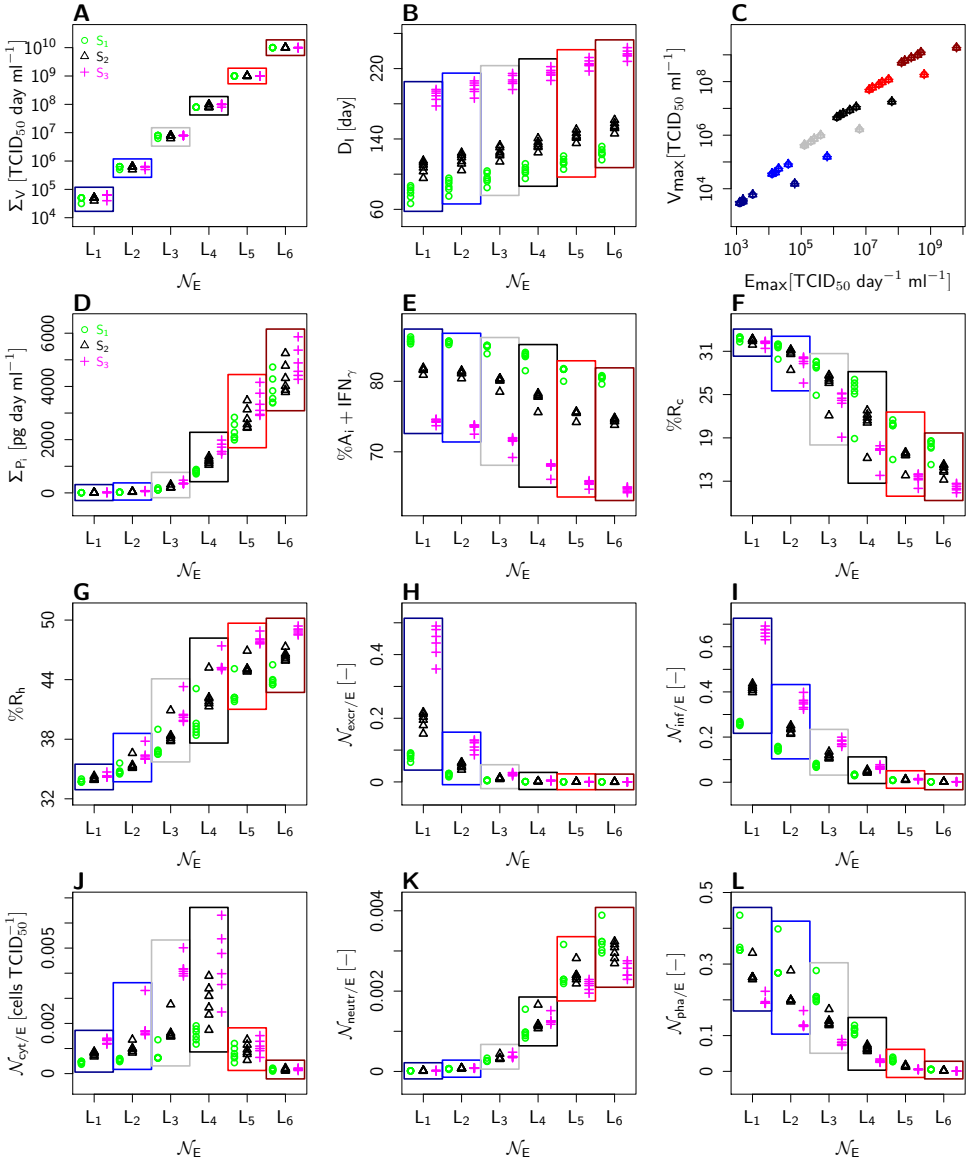

FIG. 11. **Impact of scenario parameters on viral and immune characteristics for simple exposures (design $\mathbf{D_1}$).** **A**: area under the viral curve Σ_V ; **B**: infection duration D_I; **C**: viral peak $V_{\max}$; **D**: total pro-inflammatory cytokines Σ_{Pi}; **E**: percentage of antiviral cytokines $\%(\mathrm{A}_i\text{+IFN}_\gamma)$; **F**: percentage of cellular effectors $\%\mathrm{R}_c$; **G**: percentage of humoral effectors $\%\mathrm{R}_h$; **H**: normalised number of excreted viral particles $\mathcal{N}_{\text{excr/E}}$; **I**: normalised number of viral particles having infected macrophages $\mathcal{N}_{\text{inf/E}}$; **J**: normalised number of cytolysed infected macrophages $\mathcal{N}_{\text{cyt/E}}$; **K**: normalised number of neutralised viral particles $\mathcal{N}_{\text{neutr/E}}$; **L**: normalised number of phagocyted viral particles $\mathcal{N}_{\text{pha/E}}$. All characteristics but the viral peak (all but **C**) are plotted against the exposure dose $\mathcal{N}_E \in \{L_1, L_2, L_3, L_4, L_5, L_6\}$, with the virulence level highlighted in colours: $S_{\text{vir}} \in \{\circ S_1, \triangle S_2, +S_3\}$; replicates (same $\mathcal{N}_E$ and S_{vir}) and correspond to the various exposure durations. The viral peak (**C**) is plotted against the exposure peak $E_{\max}$, with the exposure dose highlighted in colours; replicates (same $\mathcal{N}_E$) correspond to the different virulence levels and exposure durations. [–] = no unit.

TABLE 5. **Relative errors on the viral characteristics due to approximations of combined exposures by simple exposures.** Combined exposures were approximated by either (a) same: one of the simple scenario of the combination (short or prolonged); or (b) max: a short or prolonged simple exposure with the highest dose of the combination. 144 approximations were computed for each characteristic. Relative errors, defined in Equation (2.4): $\mathbf{0} \in [-5, 5]\%$; positive (underestimation by the approximated simple scenario) $+ \in]5, 100]\%$; negative (overestimation) $- \in]-5, -100]\%$, $-- \in [-200, -300]\%$, $--- \in [-800, -1100]\%$.

Combined exposures		homogeneous			heterogeneous					
		short=prolonged			short=max			prolonged=max		
intensity of short:		L_1	L_4	L_6	L_4	L_6	L_6	L_1	L_1	L_4
of prolonged:		L_1	L_4	L_6	L_1	L_1	L_4	L_4	L_6	L_6
Relative errors on the area under the viral curve $\Delta\Sigma_V$ when approximated by:										
short	same / max	$+$	$+$	$+$	$\mathbf{0}$	$\mathbf{0}$	$\mathbf{0}$	$\frac{+}{\mathbf{0}}$	$\frac{+}{\mathbf{0}}$	$\frac{+}{\mathbf{0}}$
prolonged	same / max	$+$	$+$	$+$	$\frac{+}{\mathbf{0}}$	$\frac{+}{\mathbf{0}}$	$\frac{+}{\mathbf{0}}$	$\mathbf{0}$	$\mathbf{0}$	$\mathbf{0}$
Relative errors on the infection duration ΔD_I when approximated by:										
short	same / max	$+$	$+$	$+$	$\mathbf{0}$	$\mathbf{0}$	$\mathbf{0}$	$\frac{+}{+}$	$\frac{+}{+}$	$\frac{+}{+}$
prolonged	same / max	$\mathbf{0}$	$\mathbf{0}$	$\mathbf{0}$	$\frac{+}{-}$	$\frac{+}{-}$	$\frac{+}{-}$	$\mathbf{0}$	$\mathbf{0}$	$\mathbf{0}$
Relative errors on the viral peak $\Delta V_{\max}$ when approximated by:										
short	same / max	$\mathbf{0}$	$\mathbf{0}$	$\mathbf{0}$	$\mathbf{0}$	$\mathbf{0}$	$\mathbf{0}$	$\frac{+}{--}$	$\frac{+}{--}$	$\frac{+}{--}$
prolonged	same / max	$+$	$+$	$+$	$\frac{+}{\mathbf{0}}$	$\frac{+}{\mathbf{0}}$	$\frac{+}{\mathbf{0}}$	$\mathbf{0}$	$\mathbf{0}$	$\mathbf{0}$
Relative errors on the viral peak date $\Delta T_{\max}$ when approximated by:										
short	same / max	$\mathbf{0}$	$\mathbf{0}$	$\mathbf{0}$	$\mathbf{0}$	$\mathbf{0}$	$\mathbf{0}$	$\frac{+}{--}$	$\frac{+}{--}$	$\frac{+}{--}$
prolonged	same / max	$---$	$---$	$---$	$\frac{---}{---}$	$\frac{---}{---}$	$\frac{---}{---}$	$\mathbf{0}$	$\mathbf{0}$	$\mathbf{0}$

HOMOGENEOUS COMBINATIONS The viral characteristics of the homogeneous exposure combinations (same exposure intensity for the short and prolonged exposures of the combinations) were approximated as follows (first three result columns in Table 5). The area under the viral curve Σ_V was similarly underestimated by short and prolonged exposures (positive errors). The infection duration D_I was well estimated by prolonged exposures and underestimated by short exposures. The viral peak $V_{\max}$ was well estimated by short exposures and underestimated by prolonged exposures. The viral peak date $T_{\max}$ was well estimated by short exposures and highly overestimated by prolonged exposures.

HETEROGENEOUS COMBINATIONS The viral characteristics of the heterogeneous exposure combinations were approximated as follows (six last columns in Table 5). If the highest intensity corresponds to the short (respectively prolonged) exposure of the combination, *i.e.* short=max (resp. prolonged=max) in Table 5, then approximations by short (resp. prolonged) simple exposures were very good for all viral characteristics. Otherwise, approximations generated notable errors. Σ_V was underestimated by both short and prolonged simple exposure. D_I was underestimated by short simple exposures, $V_{\max}$ by prolonged simple exposures. $T_{\max}$ was always underestimated by short simple exposures and highly overestimated by prolonged simple exposures.

To conclude, relative errors were globally lower when the approximation had the highest exposure dose of the combination. Σ_V was similarly approximated by short and prolonged simple exposures. D_I was globally better approximated by prolonged exposures. $V_{\max}$ and $T_{\max}$ were globally better approximated by short exposures. All viral characteristics tended to be underestimated, except $T_{\max}$ which tended to be highly overestimated in most cases.

4. Discussion

We studied the impact of exposure on PRRSv infection dynamics and the underlying immune mechanisms by a modelling approach. We used a deterministic within-host model describing the immune response to PRRSv infection. We represented the exposure to the virus by a bell-shaped function, characterised by its duration and intensity. We explored the influence of the exposure duration and intensity combined with the virulence level on PRRSv within-host dynamics. Our results showed that virulence level, the exposure intensity and its duration had a notable and complex impact on the viral load and the associated immune response. These results consequently provide new insights regarding the exposure influence on PRRSv spread and host protection against re-infection. Finally, they draw guidelines on how and when to take exposure into account in future experimental and modelling approaches.

4.1. Exposure has an impact on PRRSv spread and host protection

Reducing pig infectiousness and improving host protection are key measures to limit the spread of a disease. Assessing the exposure impact on both pig infectiousness and host protection is hence key issue to guide future studies on disease control.

INFECTIOUSNESS is strongly correlated with viremia (Charpin *et al.*, 2012), which can be characterised by two major indicators: the infection duration and the infection severity. Both result from the interaction between the virus and the immune response. Furthermore, PRRSv most severe infections, associated with a strong inflammation, can result in the death of the pig. So we explored the impact of PRRSv exposure on the infection duration and severity, but also on the associated immune response.

Previous studies showed that the total level of pro-inflammatory cytokines was positively correlated with infection severity (Gómez-Laguna *et al.*, 2010; Van Reeth & Nauwynck, 2000). Moreover, we found that the area under the viral curve (which is a synthetic indicator of the infection severity) and the total level of pro-inflammatory cytokines were both fully determined by the exposure dose.

In contrast, the infection duration was mainly determined by the strain virulence, but for a given strain virulence, it exhibited a positive correlation with the exposure dose and the exposure duration. Whatever the exposure and strain virulence, the infection duration decreased while the percentage of antiviral cytokines increased. These results are consistent with an experimental study on influenza, which

found that the exposure dose influenced the infection dynamics *via* the antiviral cytokines (Marois *et al.*, 2012). We also found that, in agreement with the literature, short infection durations were globally associated with the dominance of the cellular response over the humoral response for a given strain virulence (Kimman *et al.*, 2009; Lunney & Chen, 2010; Murtaugh & Genzow, 2011; Thanawongnuwech & Suradhat, 2010).

To conclude, the exposure dose and duration hence affect the pig infectiousness, which is also modulated by the strain virulence. An estimate of the viral dose received through exposure should be enough to infer the infection severity, if approximated by the area under the viral curve. However, predicting the infection duration is less straightforward: it also depends on the strain virulence, exposure duration and orientation of the immune response.

HOST PROTECTION to a secondary challenge is provided by the memory response, which derives from the adaptive immune response expressed during a primary challenge. In particular, levels of cytotoxic T lymphocytes and neutralising antibodies are the main determinants of the host protection and are consequently key targets of vaccines.

We showed that the adaptive immune response was determined by both the exposure dose and the virulence level in a complex way. The total number of cytolysed infected cells per exposure dose unit was mainly determined by the exposure dose, but also notably by the virulence level. The total number of neutralised viral particles per exposure dose unit was almost fully determined by the exposure dose. Interestingly, we showed that contrasted virulence and exposure scenarios could lead to contrasted adaptive immune responses and consequently contrasted host protections, while exhibiting similar infection durations.

In conclusion, not taking into account the exposure dose and duration in combination with the virulence level for experimental and natural PRRSv infection could lead to a wrong estimation of the health status of the animal and its protection level.

SATURATIONS FOR HIGH EXPOSURE DOSES Most key immune mechanisms known to directly affect the viral dynamics (viral excretion, cell infection, infected cell cytolysis, viral neutralisation and phagocytosis) saturated in the model for high viral exposure doses. Such saturations are fairly realistic, as the production of immune cells and the number of receptors on these cells are limited. Once the cells and their receptors are mobilised, increasing the exposure dose cannot induce a higher activation of the mechanisms.

In the model, exposure corresponds to an intake of free viral particles. Immune mechanisms involving viral particles do not integrate explicit saturations for high viral concentrations. However, these mechanisms are up- and down-regulated by various cytokines and these regulations do saturate for high cytokine concentrations (Michaelis–Menten based functions), representing the limited number of receptors on cells. Furthermore, the cytokines that regulate immune cell mechanisms are in turn produced by activated immune cells. We implemented in our model the major cytokine productions and regulations described in the literature (**Tables A1 & A2**, Supplementary material). So the activation levels of immune mechanisms, in particular the saturation effects observed for high exposure doses, depend on several interacting feedback loops, which make mechanistic explanations virtually impossible.

4.2. When and how to take PRRSv exposure into account?

IN PRRSV EXPERIMENTAL INFECTION of non-isolated pigs, the exposure due to contacts between inoculated pigs is often considered as negligible. However, there is no study which compares the within-host dynamics of isolated and non-isolated inoculated pigs. We used our model to weigh up this hypothesis. For each virulence level and each inoculum dose, we compared a short exposure scenario, representing the inoculum, with exposure scenarios combining this short exposure with several prolonged exposures, representing contacts. When the exposure dose due to contacts was lower than the inoculum dose, the infection duration and severity were similar for the short and combined scenarios. When the exposure dose due to contacts exceeded the inoculum dose, these viral characteristics became notably higher for the combined scenarios. Experimental studies showed that the higher the PRRSv strain

virulence, the higher the infectiousness of infected pigs (Johnson *et al.*, 2004; Charpin *et al.*, 2012). Moreover, we showed here and in (Go *et al.*, 2014, Go, 2014) that higher strain virulence's induced longer infections. Therefore, an experimental inoculation of non-isolated pigs with a highly virulent strain should result in a high exposure by contacts. The within-host dynamics of pigs inoculated with the same dose of a highly virulent strain, in particular their estimated infection duration and severity, would then be notably higher for non-isolated pigs than for isolated pigs.

IN MODELLING APPROACHES and particularly for immuno-epidemiological models, exposure is a key issue. Most models approximate the exposure by a punctual dose and do not further investigate its impact. We chose to study the impact of exposure by varying the characteristics of a given exposure function (a bell-shaped function). We found that the exposure intensity (the total viral dose received through exposure) and to a lesser extent the exposure duration and peak had a strong impact on the within-host dynamics, which could vary according to PRRSv strain virulence. Fixing the exposure dose, we looked at the impact of the exposure duration and peak.

Firstly, from our results on simple exposure scenarios, we deduced that approximating a prolonged exposure by a short exposure with the same exposure dose would result in (i) a good estimation of the infection severity ; (ii) an underestimation of the infection duration; and (iii) an overestimation of the viral peak and an underestimation of the viral peak date. Obviously, when approximating a prolonged exposure by short exposure, the higher the exposure duration of the prolonged exposure, the worse the errors on the within-host dynamics. As our short exposure function is a narrow bell-shaped curve, similar errors would be expected when approximating the exposure by a punctual exposure dose (initial condition).

Secondly, comparing combined exposure scenarios and simple scenarios, we showed that a short exposure was a better approximation for the viral peak and its date, whereas a prolonged exposure was a better approximation for the infection duration. The infection severity was similarly underestimated with both approximations. The approximated exposure duration would then be chosen according to which viral characteristics we would want to estimate best.

To conclude, a good approximation of the exposure should at least preserve the exposure dose, especially to estimate the infection severity. Besides, representing the exposure due to contacts by a short or even a punctual exposure would tend to underestimate the infection duration. As the infection severity and duration both contribute to the pig infectiousness, a prolonged exposure of the adequate intensity would probably be an adequate choice in an immuno-epidemiological context.

Supplementary material

Supplementary material is available in a separate file.

Acknowledgements

Financial support for this research was provided by ABIES Doctoral School, the French National Institute for Agricultural Research (INRA) and the French National Research Agency (ANR), program "Investments for the Future", project ANR-10-BINF-07 (MIHMES).

References

AIT-ALI, TAHAR, WILSON, ALISON D., CARRÉ, WILFRID, WESTCOTT, DAVID G., FROSSARD, JEAN-PIERRE, MELLENCAMP, MARNIE A., MOUZAKI, DAPHNE, MATIKA, OSWALD, WADDINGTON, DAVID, DREW, TREVOR W., BISHOP, STEPHEN C., & ARCHIBALD, ALAN L. 2011. Host inhibits replication of European porcine reproductive and respiratory syndrome virus in macrophages by altering differential regulation of type-I interferon transcriptional responses. *Immunogenetics*, **63**(7), 437–448.

BEAUCHEMIN, CATHERINE, & HANDEL, ANDREAS. 2011. A review of mathematical models of influenza A infections within a host or cell culture: lessons learned and challenges ahead. *Bmc public health*, **11**.

BEN-AMI, FRIDA, EBERT, DIETER, & REGOES, ROLAND R. 2010. Pathogen dose infectivity curves as a method to analyze the distribution of host susceptibility: a quantitative assessment of maternal effects after food stress and pathogen exposure. *The american naturalist*, **175**(1), 106–115.

BORGHETTI, PAOLO. 2005 (27–28 October). Cell-mediated immunity and viral infection in pig. *Pages 27–46 of: Prrs fatti vs speculazioni*. Università degli Studi di Parma, Dipartimento di Salute Animale, Parma, Italy.

BOSCH, ASTRID A. T. M., BIESBROEK, GISKE, TRZCINSKI, KRZYSZTOF, SANDERS, ELISABETH A. M., & BOGAERT, DEBBY. 2013. Viral and bacterial interactions in the upper respiratory tract. *Plos pathog.*, **9**(1), e1003057.

BRACIALE, THOMAS J., SUN, JIE, & KIM, TAEG S. 2012. Regulating the adaptive immune response to respiratory virus infection. *Nat. rev. immunol.*, **12**(4), 295–305.

CHARPIN, CÉLINE, MAHÉ, SOPHIE, KERANFLEC'H, ANDRÉ, BELLOC, CATHERINE, CARIOLET, ROLAND, LE POTIER, MARIE-FRÉDÉRIQUE, & ROSE, NICOLAS. 2012. Infectiousness of pigs infected by the porcine reproductive and respiratory syndrome virus (PRRSV) is time-dependent. *Vet. res.*, **43**(1), 69.

COQUERELLE, CAROLINE, & MOSER, MURIEL. 2010. DC subsets in positive and negative regulation of immunity. *Immunol. rev.*, **234**(1), 317–334.

DARWICH, LAILA, DÍAZ, IVAN, & MATEU, ENRIC. 2010. Certainties, doubts and hypotheses in porcine reproductive and respiratory syndrome virus immunobiology. *Virus res.*, **154**(1-2), 123–132.

DARWICH, LAILA, GIMENO, MARIONA, SIBILA, MARINA, DÍAZ, IVAN, DE LA TORRE, EUGENIA, DOTTI, SILVIA, KUZEMTSEVA, LIUDMILA, MARTIN, MARGARITA, PUJOLS, JOAN, & MATEU, ENRIC. 2011. Genetic and immunobiological diversities of porcine reproductive and respiratory syndrome genotype I strains. *Vet. microbiol.*, **150**(1–2), 49–62.

DOBROVOLNY, HANA M., REDDY, MICAELA B., KAMAL, MOHAMED A., RAYNER, CRAIG R., & BEAUCHEMIN, CATHERINE A. A. 2013. Assessing mathematical models of influenza infections using features of the immune response. *Plos one*, **8**(2), e57088.

DOESCHL-WILSON, ANDREA, & GALINA-PANTOJA, LUCINA. 2010. Using mathematical models to gain insight into host-pathogen interaction in mammals: porcine reproductive and respiratory syndrome. *Chap. 4, page 109–131 of:* BARTON, ANNETTE W. (ed), *Host–pathogen interactions: genetics, immunology and physiology*. Immunology and Immune System Disorders. New York, USA: Nova Science Publishers.

GAMMACK, D., GANGULI, S., MARINO, S., SEGOVIA-JUAREZ, J., & KIRSCHNER, D. 2005. Understanding the immune response in tuberculosis using different mathematical models and biological scales. *Multiscale model. sim.*, **3**(2), 312–345.

GANDOLFI, ALBERTO, PUGLIESE, ANDREA, & SINISGALLI, CARMELA. 2014. Epidemic dynamics and host immune response: a nested approach. *J. math. biol.* Online.

GIMENO, MARIONA, DARWICH, LAILA, DÍAZ, IVAN, DE LA TORRE, EUGENIA, PUJOLS, JOAN, MARTIN, MARGA, INUMARU, SHIGEKI, CANO, ESMERALDA, DOMÍNGO, MARIANO, MONTOYA, MARIA, & MATEU, ENRIC. 2011. Cytokine profiles and phenotype regulation of antigen presenting cells by genotype-I porcine reproductive and respiratory syndrome virus isolates. *Vet. res.*, **42**(9).

GO, NATACHA. 2014. *Modelling the immune response to the Porcine Respiratory and Reproductive Syndrome virus*. Ph.D. thesis, L'institut des Sciences et Industries du Vivant et de l'Environnement (AgroParisTech).

GO, NATACHA, BIDOT, CAROLINE, BELLOC, CATHERINE, & TOUZEAU, SUZANNE. 2014. Integrative model of the immune response to a pulmonary macrophage infection: what determines the infection duration? *Plos one*, **9**(9), e107818.

GÓMEZ-LAGUNA, J, SALGUERO, FJ, PALLARÉS, FJ, FERNÁNDEZ DE MARCO, M, BARRANCO, I, CERÓN, JJ, MARTÍNEZ-SUBIELA, S, VAN REETH, KRISTIEN, & CARRASCO, L. 2010. Acute phase response in porcine reproductive and respiratory syndrome virus infection. *Comp. immunol. microb.*, **33**(6), e51–e58.

GÓMEZ-LAGUNA, JAIME, SALGUERO, FRANCISCO J., PALLARÉS, FRANCISCO J., & CARRASCO, LIBRADO. 2013. Immunopathogenesis of porcine reproductive and respiratory syndrome in the respiratory tract of pigs. *Vet. j.*, **195**(2), 148–155.

HERMANN, J. R., MUNOZ-ZANZI, C. A., ROOF, M. B., BURKHART, K., & ZIMMERMAN, J. J/. 2005. Probability of porcine reproductive and respiratory syndrome (PRRS) virus infection as a function of exposure route and dose. *Vet. microbiol.*, **110**(1), 7–16.

JOHNSON, WESLEY, ROOF, MICHAEL, VAUGHN, ERIC, CHRISTOPHER-HENNINGS, JANE, JOHNSON, CRAIG R., & MURTAUGH, MICHAEL P. 2004. Pathogenic and humoral immune responses to porcine re-

productive and respiratory syndrome virus (PRRSV) are related to viral load in acute infection. *Vet. immunol. immunop.*, **102**(3), 233–247.

KIDD, PARRIS. 2003. Th1/Th2 balance: the hypothesis, its limitations, and implications for health and disease. *Altern. med. rev.*, **8**(3), 223–246.

KIMMAN, TJEERD G., CORNELISSEN, LISETTE A., MOORMANN, ROB J., REBEL, JOHANNA M. J., & STOCKHOFE-ZURWIEDEN, NORBERT. 2009. Challenges for porcine reproductive and respiratory syndrome virus (PRRSV) vaccinology. *Vaccine*, **27**(28), 3704–3718.

KNOSP, CAMILLE A., & JOHNSTON, JAMES A. 2012. Regulation of CD4+ T-cell polarization by suppressor of cytokine signalling proteins. *Immunology*, **135**(2), 101–111.

LABARQUE, G., VAN GUCHT, S., NAUWYNCK, H., VAN REETH, K., & PENSAERT, M. 2003. Apoptosis in the lungs of pigs infected with porcine reproductive and respiratory syndrome virus and associations with the production of apoptogenic cytokines. *Vet. res.*, **34**, 249–260.

LABARQUE, GEOFFREY G., NAUWYNCK, HANS J., VAN REETH, KRISTIEN, & PENSAERT, MAURICE B. 2000. Effect of cellular changes and onset of humoral immunity on the replication of porcine reproductive and respiratory syndrome virus in the lungs of pigs. *J. gen. virol.*, **81**(5), 1327–1334.

LAMBONI, MATIEYENDOU, MONOD, HERVÉ, & MAKOWSKI, DAVID. 2011. Multivariate sensitivity analysis to measure global contribution of input factors in dynamic models. *Reliab. eng. syst. safe.*, **96**(4), 450–459.

LEROITH, TANYA, & AHMED, S. ANSAR. 2012. Regulatory T cells and viral disease. *Chap. 6, pages 121–144 of:* KHATAMI, MAHIN (ed), *Inflammation, chronic diseases and cancer: Cell and molecular biology, immunology and clinical bases*. Rijeka, Croatia: InTech.

LI, YAN, & HANDEL, ANDREAS. 2014. Modeling inoculum dose dependent patterns of acute virus infections. *J. theor. biol.*, **347**, 63–73.

LIU, YONGGANG, SHI, WENDA, ZHOU, ENMIN, WANG, SHUJIE, HU, SHOUPING, CAI, XUEHUI, RONG, FULONG, WU, JIABIN, XU, MIN, XU, MINGMING, & LI, LIQIN. 2010. Dynamic changes in inflammatory cytokines in pigs infected with highly pathogenic porcine reproductive and respiratory syndrome virus. *Clin. vaccine immunol.*, **17**(9), 1439–1445.

LUNNEY, JOAN K., & CHEN, HONGBO. 2010. Genetic control of host resistance to porcine reproductive and respiratory syndrome virus (PRRSV) infection. *Virus res.*, **154**(1–2), 161–169.

LUNNEY, JOAN K., FRITZ, ERIC R., REECY, JAMES M., KUHAR, DANIEL, PRUCNAL, ELIZABETH, MOLINA, RAMON, CHRISTOPHER-HENNINGS, JANE, ZIMMERMAN, JEFFREY, & ROWLAND, RAYMOND R. R. 2010. Interleukin-8, interleukin-1β, and interferon-γ levels are linked to PRRS virus clearance. *Viral immunol.*, **23**(2), 127–134.

MARINO, SIMEONE, MYERS, AMY, FLYNN, JOANNE L., & KIRSCHNER, DENISE E. 2010. TNF and IL-10 are major factors in modulation of the phagocytic cell environment in lung and lymph node in tuberculosis: A next-generation two-compartmental model. *J. theor. biol.*, **265**(4), 586–598.

MARINO, SIMEONE, LINDERMAN, JENNIFER J., & KIRSCHNER, DENISE E. 2011. A multifaceted approach to modeling the immune response in tuberculosis. *Wiley interdiscip. rev. syst. biol. med.*, **3**(4), 479–489.

MAROIS, ISABELLE, CLOUTIER, ALEXANDRE, GARNEAU, ÉMILIE, & RICHTER, MARTIN V!;. 2012. Initial infectious dose dictates the innate, adaptive, and memory responses to influenza in the respiratory tract. *J. leukocyte biol.*, **92**(1), 107–121.

MARTCHEVA, MAIA. 2011. An immuno-epidemiological model of paratuberculosis. *Aip conf. proc.*, **1404**(1), 176–183. In *Application of Mathematics in Technical and Natural Sciences: 3rd International Conference AMiTaNS'11: Albena, Bulgaria, 20-25 June 2011*; edited by Todorov M.D. and Christov C.I.

MATEU, E., & DÍAZ, I. 2008. The challenge of PRRS immunology. *Vet. j.*, **177**, 345–351.

MIDEO, NICOLE, ALIZON, SAMUEL, & DAY, TROY. 2008. Linking within-and between-host dynamics in the evolutionary epidemiology of infectious diseases. *Trends ecol. evol.*, **23**(9), 511–517.

MURILLO, LISA N., MURILLO, MICHAEL S., & PERELSON, ALAN S. 2013. Towards multiscale modeling of influenza infection. *J. theor. biol.*, **332**, 267–290.

MURTAUGH, MICHAEL P. 2004 (6–9 March). PRRS immunology: what are we missing? *Pages 359–367 of: 35th annual meeting of the american association of swine veterinarians*.

MURTAUGH, MICHAEL P. 2005 (27–28 October). PRRSV/host interaction. *Pages 73–80 of: Prrs fatti vs speculazioni*. Università degli Studi di Parma, Dipartimento di Salute Animale, Parma, Italy.

MURTAUGH, MICHAEL P., & GENZOW, MARIKA. 2011. Immunological solutions for treatment and prevention of porcine reproductive and respiratory syndrome (PRRS). *Vaccine*, **29**(46), 8192–8204.

NAUWYNCK, H. J., VAN GORP, H., VANHEE, M., KARNIYCHUK, U., GELDHOF, M., CAO, A., VERBEECK, M., & VAN BREEDAM, W. 2012. Micro-dissecting the pathogenesis and immune response of PRRSV infection paves the way for more efficient PRRSV vaccines. *Transbound. emerg. dis.*, **59**, 50–54.

PEPIN, K. M., VOLKOV, I., BANAVAR, J. R., WILKE, C. O., & GRENFELL, B. T. 2010. Phenotypic differences in viral immune escape explained by linking within-host dynamics to host-population immunity. *J. theor. biol.*, **265**(4), 501–510.

PETRY, D. B., LUNNEY, J., BOYD, P., KUHAR, D., BLANKENSHI, E., & JOHNSON, R. K. 2007. Differential immunity in pigs with high and low responses to porcine reproductive and respiratory syndrome virus infection. *J. anim. sci.*, **85**, 2075–2092.

PUJOL, JOSEP M, EISENBERG, JOSEPH E, HAAS, CHARLES N, & KOOPMAN, JAMES S. 2009. The effect of ongoing exposure dynamics in dose response relationships. *Plos comput biol*, **5**(6), e1000399.

ROUSE, BARRY T., & SEHRAWAT, SHARVAN. 2010. Immunity and immunopathology to viruses: what decides the outcome? *Nat. rev. immunol.*, **10**(7), 514–526.

SALTELLI, A., CHAN, K., & SCOTT, E. M. (eds). 2000. *Sensitivity analysis*. Wiley Series in Probability and Statistics. Chichester, UK: Wiley.

SMITH, AMBER M., & PERELSON, ALAN S. 2011. Influenza A virus infection kinetics: quantitative data and models. *Wiley interdiscip. rev. syst. biol. med.*, **3**(4), 429–445.

STEINMEYER, SHELBY H, WILKE, CLAUS O, & PEPIN, KIM M. 2010. Methods of modelling viral disease dynamics across the within-and between-host scales: the impact of virus dose on host population immunity. *Philos t. r. soc. b*, **365**(1548), 1931–1941.

THANAWONGNUWECH, ROONGROJE, & SURADHAT, SANIPA. 2010. Taming PRRSV: Revisiting the control strategies and vaccine design. *Virus res.*, **154**(1-2), 133–140.

VAN REETH, KRISTIEN, & NAUWYNCK, HANS. 2000. Proinflammatory cytokines and viral respiratory disease in pigs. *Vet. res.*, **31**(2), 187–213.

WESLEY, D. R., LAGER, K. M., & KEHRLI, M. E. 2006. Infection with porcin reproductive and respiratory syndrome virus stimulates an early gamma interferon response in the serum of pig. *Can. j. vet. res.*, **70**(3), 176–182.

WIGGINTON, JANIS E., & KIRSCHNER, DENISE. 2001. A model to predict cell-mediated immune regulatory mechanisms during human infection with Mycobacterium tuberculosis. *J. immunol.*, **166**, 1951–1967.

YOO, DONGWAN, SONG, CHENG, SUN, YAN, DU, YIJUN, KIM, OEKYUNG, & LIU, HSIAO-CHING. 2010. Modulation of host cell responses and evasion strategies for porcine reproductive and respiratory syndrome virus. *Virus res.*, **154**(1–2), 48–60.

YOON, KYOUNG-JIN, ZIMMERMAN, JEFFREY J., CHANG, CHIH-CHENG, CANCEL-TIRADO, SOL, HARMON, KAREN M., & MCGINLEY, MICHAEL J. 1999. Effect of challenge dose and route on porcine reproductive and respiratory syndrome virus (PRRSV) infection in young swine. *Vet. res.*, **30**(6), 629–638.

ZIMMERMAN, J., BENFIELD, D. A., MURTAUGH, M. P., OSORIO, F., STEVENSON, G. W., & TORREMORELL, M. 2006. Porcine reproductive and respiratory syndrome virus (porcine arterivirus). *Chap. 24, pages 387–418 of:* STRAW, B. E., ZIMMERMAN, J. J., D'ALLAIRE, S., & TAYLOR, D. L. (eds), *Diseases of swine*, ninth edn. Oxford, UK: Blackwell.